https://doi.org/10.5194/hess-2019-346
Preprint. Discussion started: 10 September 2019


Hydrology and Earth System Sciences
Discussions

# Using altimetry observations combined with GRACE to select parameter sets of a hydrological model in data scarce regions

Petra Hulsman[1], Hessel C. Winsemius[1], Claire Michailovsky[2], Hubert H.G. Savenije[1], Markus Hrachowitz[1]

[1]Water Resources Section, Faculty of Civil Engineering and Geosciences, Delft University of Technology, Stevinweg 1, 2628 CN Delft, The Netherlands
[2]IHE Delft Institute for Water Education, Westvest 7, 2611 AX Delft, The Netherlands

*Correspondence to*: Petra Hulsman (p.hulsman@tudelft.nl)

**Abstract.** To ensure reliable model understanding of water movement and distribution in terrestrial systems, sufficient and good quality hydro-meteorological data are required. Limited availability of ground measurements in the vast majority of river basins world-wide increase the value of alternative data sources such as satellite observations in modelling. In the absence of directly observed river discharge data, other variables such as remotely sensed river water level may provide valuable information for the calibration and evaluation of hydrological models. This study investigates the potential of the use of remotely sensed river water level, i.e. altimetry observations, from multiple satellite missions to identify parameter sets for a hydrological model in the semi-arid Luangwa River Basin in Zambia. A distributed process-based rainfall runoff model with sub-grid process heterogeneity was developed and run on a daily timescale for the time period 2002 to 2016. Following a step-wise approach, various parameter identification strategies were tested to evaluate the potential of satellite altimetry data for model calibration. As a benchmark, feasible model parameter sets were identified using traditional model calibration with observed river discharge data. For the parameter identification using remote sensing, data from the Gravity Recovery and Climate Experiment (GRACE) were used in a first step to restrict the feasible parameter sets based on the seasonal fluctuations in total water storage. In a next step, three alternative ways of further restricting feasible model parameter sets based on satellite altimetry time-series from 18 different locations, i.e. virtual stations, along the Luangwa River and its tributaries were compared. In the calibrated benchmark case, daily river flows were reproduced relatively well with an optimum Nash-Sutcliffe efficiency of $E_{NS,Q}$ = 0.78 (5/95$^{th}$ percentiles of all feasible solutions $E_{NS,Q,5/95}$ = 0.61 – 0.75). When using only GRACE observations to restrict the parameter space, assuming no discharge observations are available, an optimum of $E_{NS,Q}$ = -1.4 ($E_{NS,Q,5/95}$ = -2.3 – 0.38) with respect to discharge was obtained. Depending on the parameter selection strategy, it could be shown that altimetry data can contain sufficient information to efficiently further constrain the feasible parameter space. The direct use of altimetry based river levels frequently over-estimated the flows and poorly identified feasible parameter sets due to the non-linear relationship between river water level and river discharge ($E_{NS,Q,5/95}$ = -2.9 – 0.10); therefore, this strategy was of limited use to identify feasible model parameter sets. Similarly, converting modelled discharge into water levels using rating curves in the form of power relationships with two additional free calibration parameters per virtual station resulted in an over-estimation of the discharge and poorly identified feasible parameter sets ($E_{NS,Q,5/95}$ = -2.6 – 0.25). However, accounting for river geometry proved to be highly effective; this included using river cross-section and gradient information extracted from global high-resolution terrain data available on Google Earth, and applying the Strickler-Manning equation with effective roughness as free calibration parameter to convert

https://doi.org/10.5194/hess-2019-346
Preprint. Discussion started: 10 September 2019


Hydrology and Earth System Sciences
Discussions
Open Access
EGU

modelled discharge into water levels. Many parameter sets identified with this method reproduced the hydrograph and multiple other signatures of discharge reasonably well with an optimum of $E_{NS,Q}$ = 0.60 ($E_{NS,Q,5/95}$ = -0.31 – 0.50). It was further shown that more accurate river cross-section data improved the water level simulations, modelled rating curve and discharge simulations during intermediate and low flows at the basin outlet at which detailed on-site cross-section information was available. For this case, the Nash-Sutcliffe efficiency with respect to river water levels increased from $E_{NS,SM,GE}$ = -1.8 ($E_{NS,SM,GE,5/95}$ = -6.8 – -3.1) using river geometry information extracted from Google Earth to $E_{NS,SM,ADCP}$ = 0.79 ($E_{NS,SM,ADCP,5/95}$ = 0.6 – 0.74) using river geometry information obtained from a detailed survey in the field. It could also be shown that increasing the number of virtual stations used for parameter selection in the calibration period can considerably improve the model performance in spatial split sample validation. The results provide robust evidence that in the absence of directly observed discharge data for larger rivers in data scarce regions, altimetry data from multiple virtual stations combined with GRACE observations have the potential to fill this gap when combined with readily available estimates of river geometry, thereby allowing a step towards more reliable hydrological modelling in poorly or ungauged basins.

## 1 Introduction

Reliable models of water movement and distribution in terrestrial systems require sufficient good quality hydro-meteorological data throughout the modelling process. However, the development of robust models is challenged by the limited availability of ground measurements in the vast majority of river basins world-wide (Hrachowitz et al., 2013). Therefore, modellers increasingly resort to alternative data sources such as satellite data (Lakshmi, 2004;Winsemius et al., 2008;Sun et al., 2018;Pechlivanidis and Arheimer, 2015;Demirel et al., 2018;Zink et al., 2018;Rakovec et al., 2016;Nijzink et al., 2018).

In the absence of directly observed river discharge data, various types of remotely sensed variables provide valuable information for the calibration and evaluation of hydrological models. These include, for instance, remotely sensed time series of river width (Sun et al., 2012;Sun et al., 2015), flood extent (Montanari et al., 2009;Revilla-Romero et al., 2015), or river or lake water levels, i.e. altimetry (Getirana et al., 2009;Getirana, 2010;Sun et al., 2012;Garambois et al., 2017;Pereira-Cardenal et al., 2011;Velpuri et al., 2012).

Satellite altimetry observations provide estimates of the water level relative to a reference ellipsoid. For these observations, a radar signal is emitted from the satellite in the nadir direction and reflected back by the earth surface; the time difference between sending and receiving this signal is then used to estimate the distance between the satellite and the earth surface. As the position of the satellite is known at very high accuracy, this distance can then be used to infer the surface level relative to a reference ellipsoid (Łyszkowicz and Bernatowicz, 2017;Calmant et al., 2009). Satellite altimetry is sensed and recorded along the satellite's track. Altimetry based water levels can therefore only be observed where these tracks intersect with open-water surfaces; for rivers, these points are typically referred to as "virtual stations" (de Oliveira Campos et al., 2001;Birkett, 1998;Schneider et al., 2017;Jiang et al., 2017;Seyler et al., 2013). Depending on the satellite mission, the equatorial inter-track distance can vary between 75 km and 315 km, the along-track distance between 173 m and 374 m, and the temporal resolution between 10 days and 35 days (Schwatke et al., 2015;CNES, Accessed 2018;ESA, 2018;Łyszkowicz and Bernatowicz, 2017). Due to this rather coarse resolution, the application of remotely sensed altimetry data is at this moment limited to large lakes or rivers of

https://doi.org/10.5194/hess-2019-346
Preprint. Discussion started: 10 September 2019


Hydrology and Earth System Sciences
Discussions

more than approximately 200 m wide (Getirana et al., 2009;de Oliveira Campos et al., 2001;Biancamaria et al., 2017). Use of altimetry for hydrological models so far also remains rather rare due to the relatively low temporal resolution of the data, with applications typically limited to monthly or longer modelling time steps (Birkett, 1998).

In some previous studies, altimetry data were used to estimate river discharge at virtual stations in combination with routing models (Michailovsky and Bauer-Gottwein, 2014;Michailovsky et al., 2013) or stochastic models (Tourian et al., 2017). Other studies either directly related river altimetry to modelled discharge (Getirana et al., 2009;Getirana and Peters-Lidard, 2013;Leon et al., 2006;Paris et al., 2016) or they relied on rating curves developed with water level data from either in-situ measurements (Michailovsky et al., 2012;Tarpanelli et al., 2013;Papa et al., 2012;Tarpanelli et al., 2017) or, alternatively, from altimetry data (Kouraev et al., 2004). In typical applications, radar altimetry data from one single or only a few virtual stations were used for model calibration, validation or data assimilation; these data were mostly obtained from a single satellite mission, either TOPES/Poseison or Envisat (Sun et al., 2012;Getirana, 2010;Liu et al., 2015;Pedinotti et al., 2012;Fleischmann et al., 2018;Michailovsky et al., 2013;Bauer-Gottwein et al., 2015).

Despite these recent advances in using river altimetry in hydrological studies, exploitation of its potential is still limited. Various previous studies have argued and provided evidence based on observed discharge data that, in a special case of multi-criteria calibration, the simultaneous model calibration to flow in multiple sub-basins of a river basin, can be beneficial for a more robust selection of parameter sets and thus for a more reliable representation of hydrological processes and spatial pattern thereof (e.g. Ajami et al., 2004;Clark et al., 2016;Hrachowitz and Clark, 2017;Hasan and Pradhanang, 2017;Santhi et al., 2008). Hence, there may be considerable value in simultaneously using altimetry data not only from one single satellite mission but in combining data from multiple missions, which has not yet been systematically explored. While promising calibration results using data from Envisat were found by Getirana (2010) in tropical and Liu et al. (2015) in snow-dominated regions, altimetry data from multiple sources has not yet been used to calibrate hydrological models in semi-arid regions.

Therefore, the overarching objective of this study is to explore the combined information content (cf. Beven, 2008) of river altimetry data from multiple satellite missions and thus its potential to identify feasible parameter sets for the calibration of hydrological models of large river systems in a semi-arid, data scarce region.

In a step-wise approach we compare three parameter identification strategies using altimetry data from multiple virtual stations simultaneously against a traditional calibration approach based on observed discharge at the outlet using a distributed process-based rainfall-runoff model with sub-grid process heterogeneity for the Luangwa River basin. We test the following research hypotheses: 1) the use of altimetry data allows a meaningful selection of feasible model parameter sets to reproduce river discharge, and 2) the combined application of multiple virtual stations from multiple satellite missions improves the model's realism.

## 2 Site description

The study area is the Luangwa River in Zambia, a tributary of the Zambezi River (Figure 1). It has a basin area of 159,000 km$^2$ which is about 10% of the Zambezi River Basin. The Luangwa Basin is poorly gauged, mostly unregulated and sparsely populated with about 1.8 million inhabitants in 2005 (The World Bank, 2010). The mean annual precipitation is around 970 mm yr$^{-1}$, potential evaporation is around 1555 mm yr$^{-1}$ and river runoff

https://doi.org/10.5194/hess-2019-346
Preprint. Discussion started: 10 September 2019




reaches about 100 mm $yr^{-1}$ (The World Bank, 2010). The main land cover consists of broadleaf deciduous forest (55%), shrub land (25%) and savanna grassland (16%) (GlobCover, 2009). The irrigated area in the basin is limited to about 180 $km^2$, i.e. roughly 0.1% of the basin area with an annual water use of about 0.7 mm $yr^{-1}$ which amounts to < 0.001% of the annual basin water balance (The World Bank, 2010). The landscape varies between low lying flat areas along the river to large escarpments mostly in the North West of the basin and highlands with an elevation difference up to 1850 m (see Figure 1B and Section 3.2 for more information on the landscape classification). During the dry season, the river meanders between sandy banks while during the wet season from November to May it can cover flood plains several kilometres wide.

The Luangwa drains into the Zambezi downstream of the Kariba Dam and upstream of the Cahora Bassa Dam. The operation of both dams is crucial for hydropower production, and flood and drought protection, but is very difficult due to the lack of information from poorly gauged tributaries such as the Luangwa (SADC, 2008;Schleiss and Matos, 2016;The World Bank, 2010). As a result, the local population has suffered from severe floods and droughts (ZAMCOM et al., 2015;Beilfuss and dos Santos, 2001;Hanlon, 2001;SADC, 2008;Schumann et al., 2016).

### 2.1 Data availability

#### 2.1.1 In-situ discharge and water level observations

In the Luangwa basin, historical in-situ daily discharge and water level observations were available from the Zambian Water Resources Management Authority at the Great East Road Bridge gauging station, located at 30° 13' E and 14° 58' S (Figure 1) about 75 km upstream of the confluence with the Zambezi. In this study, all complete hydrological years of discharge data within the time period 2002 to 2016 were used; these are the years 2004, 2006 and 2008.

#### 2.1.2 Gridded data products

Besides the above in-situ observations, several gridded data products were used in this study for topographic description, model forcing (precipitation and temperature), and model parameter selection/calibration (total water storage anomalies), as shown in Table 1. The temperature data was used to estimate the potential evaporation according to the Hargreaves method (Hargreaves and Samani, 1985;Hargreaves and Allen, 2003).

**Table 1: Gridded data products used in this study**

| | Time period | Time resolution | Spatial resolution | Product name | Source |
|---|---|---|---|---|---|
| **Digital elevation map** | NA | NA | 0.02° | GMTED | (Danielson and Gesch, 2011) |
| **Precipitation** | 2002 – 2016 | Daily | 0.05° | CHIRPS | (Funk et al., 2014) |
| **Temperature** | 2002 – 2016 | Monthly | 0.5° | CRU | (University of East Anglia Climatic Research Unit et al., 2017) |
| **Total water storage** | 2002 – 2016 | Monthly | 1° | GRACE | (Swenson, 2012;Swenson and Wahr, 2006;Landerer and Swenson, 2012) |

https://doi.org/10.5194/hess-2019-346
Preprint. Discussion started: 10 September 2019


Hydrology and Earth System Sciences
Discussions

### 2.1.3 Altimetry data

The altimetry data used in this study was obtained from the following sources: the Database for Hydrological Time Series of Inland Waters (DAHITI; https://dahiti.dgfi.tum.de/en/) (Schwatke et al., 2015), HydroSat (http://hydrosat.gis.uni-stuttgart.de/php/index.php) (Tourian et al., 2013), Laboratoire d'Etudes en Géophysique et Océanographie Spatiales (LEGOS; http://www.legos.obs-mip.fr/soa/hydrologie/hydroweb/; see supplements for more information), and the Earth and Planetary Remote Sensing Lab (EAPRS; http://www.cse.dmu.ac.uk/EAPRS/). In total, altimetry data was obtained for 18 virtual stations in the Luangwa basin (Figure 1A) for the time period 2002 – 2016 from the satellite missions Jason 1 – 3, Envisat and Saral (Table 2, Figure S2).

**Table 2: Overview of the altimetry data in the Luangwa River Basin used in this study**

| Nr. | Longitude | Latitude | Time period | Nr. of days with data | Source | Mission | Space Agency | Temporal resolution | Equatorial inter-track distance | Along-track distance | Literature |
|---|---|---|---|---|---|---|---|---|---|---|---|
| 1 | 30.2823° | -14.8664° | 2008-2016 | 246 | DAHITI | Jason 2, 3 | NASA/CNES | 10 days | 315 km | 294 m | (Schwatke et al., 2015;CNES, Accessed 2018) |
| 2 | 30.0864° | -14.366° | 2008-2015 | 92 | DAHITI | Jason 2, 3 | | | | | |
| 3 | 32.1715° | -12.4123° | 2008-2016 | 248 | DAHITI | Jason 2, 3 | | | | | |
| 4 | 31.1868° | -13.5927° | 2002-2016 | 104 | DAHITI | Envisat, Saral | ESA (Envisat), ISRO/CNES (Saral) | 35 days | 80 km (Envisat), 75 km (Saral) | 374 m (Envisat), 173 m (Saral) | (Schwatke et al., 2015;ESA, 2018;CNES, Accessed 2018) |
| 5 | 31.6984° | -13.2039° | 2002-2016 | 82 | DAHITI | Envisat, Saral | | | | | |
| 6 | 32.2998° | -12.2007° | 2002-2016 | 100 | DAHITI | Envisat, Saral | | | | | |
| 7 | 32.2805° | -12.1157° | 2002-2016 | 103 | DAHITI | Envisat, Saral | | | | | |
| 8 | 32.831° | -11.3674° | 2002-2016 | 105 | DAHITI | Envisat, Saral | | | | | |
| 9 | 30.2704° | -14.8809° | 2008-2015 | 247 | HydroSat | Jason 2 | NASA/CNES | 10 days | 315 km | 294 m | (Tourian et al., 2016;Tourian et al., 2013) |
| 10 | 31.78405° | -13.0995° | 2002-2010 | 65 | EAPRS | Envisat | ESA | 35 days | 80 km | 374 m | (Michailovsky et al., 2012;ESA, 2018) |
| 11 | 31.71099° | -13.1943° | 2002-2010 | 93 | EAPRS | Envisat | | | | | |
| 12 | 30.2740° | -14.8763° | 2008-2015 | 231 | LEGOS | Jason 3 | NASA/CNES | 10 days | 315 km | 294 m | (Frappart et al., 2015;CNES, Accessed 2018) |
| 13 | 32.15843° | -12.412° | 2016-2016 | 28 | LEGOS | Jason 3 | | | | | |
| 14 | 32.15989° | -12.4127° | 2002-2009 | 137 | LEGOS | Jason 1 | | | | | |
| 15 | 30.2740° | -14.8763° | 2008-2016 | 271 | LEGOS | Jason 2 | | | | | |
| 16 | 32.16056° | -12.4125° | 2008-2016 | 283 | LEGOS | Jason 2 | | | | | |
| 17 | 31.80001° | -13.0909° | 2013-2016 | 35 | LEGOS | Saral | ISRO/CNES | 35 days | 75 km | 173 m | |
| 18 | 30.61577° | -14.1852° | 2013-2016 | 24 | LEGOS | Saral | | | | | |

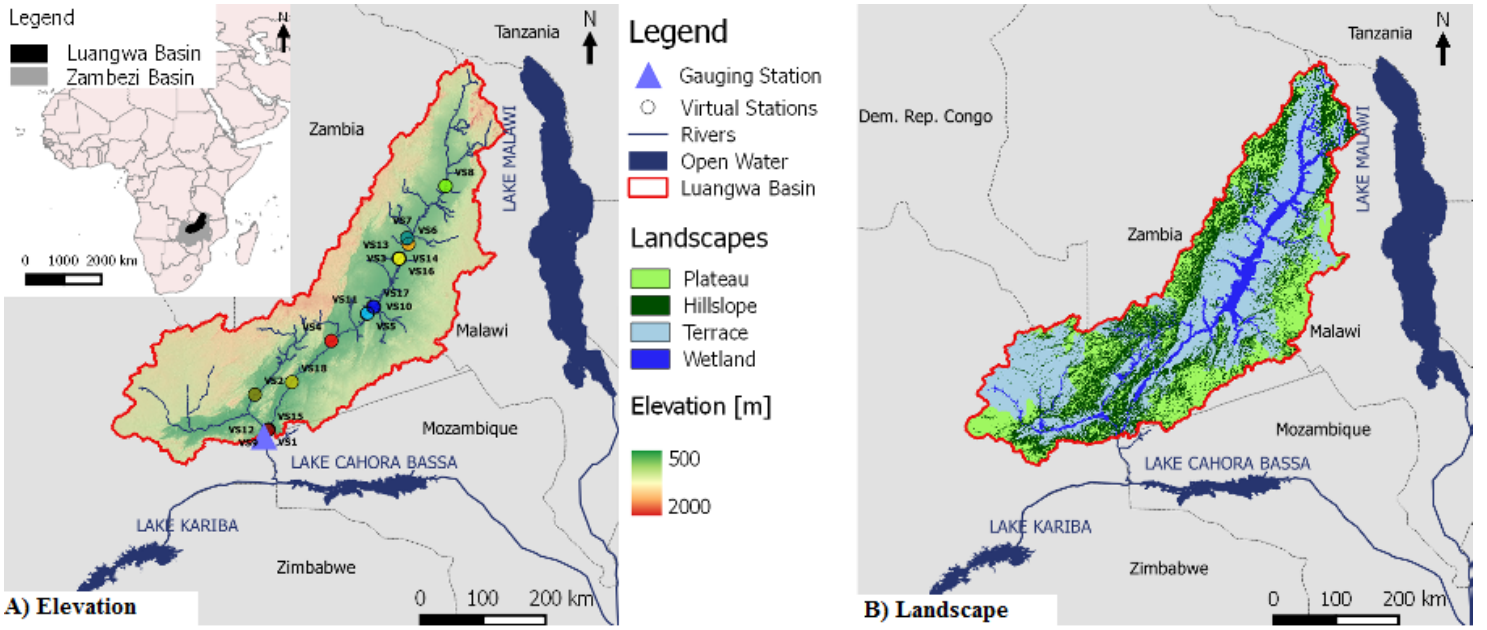


**Figure 1: A) Elevation map of the Luangwa River Basin in Zambia including the Great East Road Bridges river gauging station and the locations of the 18 virtual stations (VS 1 – VS 18) with altimetry data used in this study; their colours correspond to those in Figure 3. B) Map of the Luangwa River Basin with the main landscape types (see Section 3.2).**

https://doi.org/10.5194/hess-2019-346
Preprint. Discussion started: 10 September 2019


Hydrology and Earth System Sciences
Discussions

#### 2.1.4 River geometry information

In the Luangwa Basin, very limited detailed in-situ information was available on the river geometry such as cross-section and slope. For that reason, this information was extracted from global high-resolution terrain data available on Google Earth as done successfully in previous studies for other purposes (Pandya et al., 2017;Zhou and Wang, 2015). This was done for each virtual station and the basin outlet. Google Earth only provides river geometry information above the river water level. As the Luangwa is a perennial river, parts of the cross-section remain submerged throughout the year and thus unknown. To limit uncertainties arising from that, the cross-section geometry for each virtual station was therefore extracted from the Google Earth image with the lowest water levels at each individual virtual station. The dates of these images in general fall into the dry season, with flows at the Great East Road Bridges gauging station on the respective days ranging from 1% to 4% relative to the maximum discharge (see Supplementary Table S3 for the dates of the satellite images and the associated flows at the Great East Road Bridges gauging station). The database underlying the global terrain images in Google Earth originate from multiple, merged data sources with varying spatial resolutions. For the Luangwa Basin these include the Shuttle Radar Topography Mission (SRTM) with a spatial resolution of 30 m, the Landsat 8 with a spatial resolution of 15 m and the Satellite Pour l'Observation de la Terre 4/5 (SPOT) with a spatial resolution of 2.5 m to 20 m (Smith and Sandwell, 2003;Irons et al., 2012;Drusch et al., 2012).

In addition to Google Earth data, the submerged part of the channel cross-section was surveyed in the field on April 27$^{th}$ 2018 near the Great East Road Bridges river gauging station at the coordinates 30$^{o}$ 13' E and 15$^{o}$ 00' S (Abas, 2018) with an Acoustic Doppler Current Profiler (ADCP).

## 3 Hydrological model development

### 3.1 General approach

The potential of river altimetry for model calibration was tested with a process-based hydrological model for the Luangwa river basin. This model relied on distributed forcing allowing for spatially explicit distributed water storage calculations. The model was run on a daily time scale for the time period 2002 to 2016. To reach the objective of this study, the following distinct parameter identification strategies were compared in a stepwise approach: (1) traditional model calibration to observed river flow as benchmark; (2) identification of parameter sets reproducing the seasonal water storage anomalies based on GRACE data only; (3a) Altimetry Strategy 1: identification of parameter sets directly based on remotely sensed water levels combined with GRACE data; (3b) Altimetry Strategy 2: identification of parameter sets based on remotely sensed water levels by converting modelled discharges into water levels using calibrated rating curves combined with GRACE data; (3c) Altimetry Strategy 3: identification of parameter sets based on remotely sensed water levels by converting modelled discharges into water levels using the Strickler-Manning equation and including river geometry information (cross-section and gradient) extracted from Google Earth combined with GRACE data; (4a) Water level Strategy 1: identification of parameter sets based on daily river water level at the catchment outlet only using the Strickler-Manning equation and including river geometry information extracted from Google Earth combined with GRACE data; and (4b) Water level Strategy 2: identification of parameter sets based on daily river water level at the catchment outlet only using the Strickler-Manning equation and including river geometry

https://doi.org/10.5194/hess-2019-346
Preprint. Discussion started: 10 September 2019




information obtained from a detailed field survey with an Acoustic Doppler Current Profiler (ADCP) combined with GRACE data. Note that (1) is completely independent of (2) to (4) where no discharge data was used for the identification of parameter sets.

### 3.2 Hydrological model structure

In this study, a process-based rainfall-runoff with distributed water accounting and sub-grid process heterogeneity was developed (Ajami et al., 2004;Euser et al., 2015). The river basin was discretized into a grid with a spatial resolution of 10 x 10 $km^2$. Each model grid cell was characterized by the same model structure and parameter sets but forced by spatially distributed, gridded input data (Table 1). Runoff was then calculated in parallel for each cell separately. Subsequently, a routing scheme was applied to estimate the aggregated flow in each grid cell at each time step.

Adopting the FLEX-Topo modelling concept (Savenije, 2010) and extending it to a gridded implementation, each grid cell was further discretised into functionally distinct hydrological response classes as demonstrated by Nijzink et al. (2016). Each point within a grid cell was assigned to a response class based on its position in the landscape as defined by its local slope and "Height-above-the-nearest-drainage" (HAND; Rennó et al., 2008;Gharari et al., 2011). Similar to previous studies (e.g. Gao et al., 2016;Nijzink et al., 2016) here the response classes plateau, hillslope, terrace and wetlands were distinguished. Reflecting earlier work (e.g. Gharari et al., 2011), all locations with slope of > 4% were assumed to be hillslope. Locations with slopes lower than that were then either defined as wetland (HAND < 11m), terrace (11m ≤ HAND < 275m) or plateau (HAND ≥ 275m); see Figure 2. Following this classification wetlands make up 8%, terraces 41%, hillslopes 28% and plateaus 23% of the total Luangwa River Basin area as mapped in Figure 1B.

Each response class consisted of a series of storage components that are linked by fluxes. The flow generated from each grid cell at any given time step is then computed as the area-weighted flow from the individual response classes plus a contribution from the common groundwater component which connects the response classes (Figure 2). Finally, the outflow from each modelling cell was routed to downstream cells following the flow direction as extracted from the digital elevation model and a calibrated effective flow velocity to obtain the accumulated flow in each grid cell at any given time step. The relevant model equations are given in Table 3. This concept was previously successfully applied in a wide range of environments (Gao et al., 2014;Gharari et al., 2014;Fovet et al., 2015;Nijzink et al., 2016;Prenner et al., 2018).

https://doi.org/10.5194/hess-2019-346
Preprint. Discussion started: 10 September 2019


Hydrology and Earth System Sciences
Discussions
Open Access
EGU

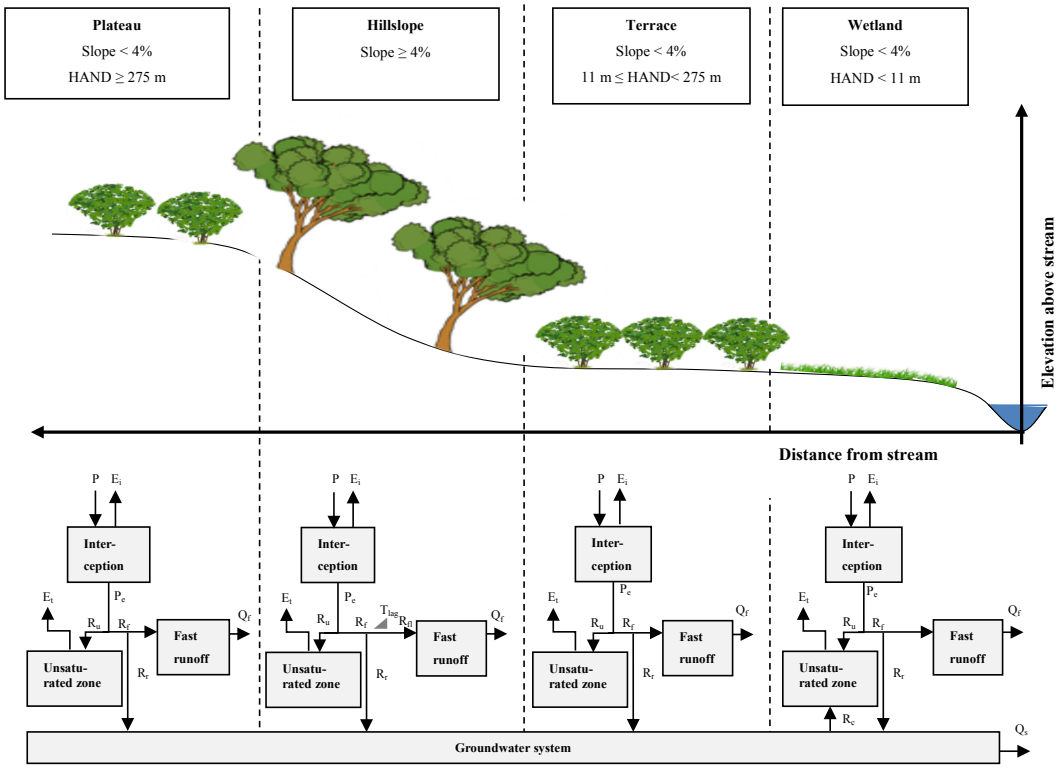


230 **Figure 2: Sketch of the hydrological response classes including the thresholds used in this analysis for the slope and HAND (Height Above Nearest Drainage) and including their corresponding model structures. This spatial sub-grid discretization was applied to each grid cell. Symbol explanation: precipitation ($P$), effective precipitation ($P_e$), interception evaporation ($E_i$), plant transpiration ($E_a$), infiltration into the unsaturated root zone ($R_u$), drainage to fast runoff component ($R_f$), delayed fast runoff ($R_{fl}$), lag time ($T_{lag}$), groundwater recharge ($R_r$), upwelling groundwater flux ($R_c$), fast runoff ($Q_f$), groundwater/slow runoff ($Q_s$).**

https://doi.org/10.5194/hess-2019-346
Preprint. Discussion started: 10 September 2019


Hydrology and Earth System Sciences
Discussions
Open Access
EGU

**Table 3: Equations applied in the hydrological model. Fluxes [mm d$^{-1}$]: precipitation ($P$), effective precipitation ($P_e$), potential evaporation ($E_p$), interception evaporation ($E_i$), plant transpiration ($E_t$), infiltration into the unsaturated zone ($R_u$), drainage to fast runoff component ($R_f$), delayed fast runoff ($R_{fl}$), groundwater recharge ($R_r$), upwelling groundwater ($R_c$), fast runoff ($Q_f$), groundwater/slow runoff ($Q_s$), total runoff ($Q_m$). Storages [mm]: storage in interception reservoir ($S_i$), storage in unsaturated root zone ($S_u$), storage in groundwater/slow reservoir ($S_s$), storage in fast reservoir ($S_f$). Parameters: interception capacity ($I_{max}$) [mm], maximum upwelling groundwater ($C_{max}$) [mm d$^{-1}$], maximum root zone storage capacity ($S_{umax}$) [mm], splitter ($W$) [-], shape parameter ($\beta$) [-], transpiration coefficient ($C_e$) [-], time lag ($T_{lag}$) [d], reservoir time scales [d] of fast ($K_f$) and slow ($K_s$) reservoirs, areal weights ($p_{HRU}$) [-],time step ($\Delta t$) [d]. Model parameters are shown in bold letters in the table below. The equations were applied to each hydrological response unit (HRU) unless indicated differently.**

| Reservoir system | Water balance equation | Process functions |
|---|---|---|
| **Interception** | $\frac{\Delta S_i}{\Delta t} = P - P_e - E_i \approx 0$ | $E_i = \min\left(E_p, \min\left(P, \frac{\boldsymbol{I_{max}}}{\Delta \boldsymbol{t}}\right)\right)$<br>$P_e = P - E_i$ |
| **Unsaturated zone** | Plateau/Hillslope/Terrace:<br>$\frac{\Delta S_u}{\boldsymbol{\Delta t}} = R_u - E_t$<br>Wetland:<br>$\frac{\Delta S_u}{\boldsymbol{\Delta t}} = R_u - E_t + R_c$ | $E_t = \min((E_p - E_i), \min\left(\frac{S_u}{\boldsymbol{\Delta t}}, (E_p - E_i) \cdot \frac{S_u}{\boldsymbol{S_{u,max}}} \cdot \frac{1}{\boldsymbol{C_e}}\right))$<br>$R_c = \min\left(\left(1 - \frac{S_u}{\boldsymbol{S_{u,max}}}\right) \cdot \boldsymbol{C_{max}}, \frac{\frac{S_s}{\Delta t}}{\boldsymbol{p_{HRU}}}\right)$<br>if $S_u + R_c \cdot \boldsymbol{\Delta t} > \boldsymbol{S_{u,max}}$ : $R_c = \frac{\boldsymbol{S_{u,max}} - S_u}{\boldsymbol{\Delta t}}$<br>Plateau/Terrace/Wetland:<br>$R_u = P_e$<br>Hillslope:<br>$R_u = (1 - C) \cdot P_e$<br>$C = 1 - \left(1 - \frac{S_u}{\boldsymbol{S_{u,max}}}\right)^{\boldsymbol{\beta}}$ |
| **Fast runoff** | $\frac{\Delta S_f}{\boldsymbol{\Delta t}} = R_{fl} - Q_f$ | $Q_f = \frac{S_f}{\boldsymbol{K_f}}$<br>Terrace/Wetland:<br>$R_f = \frac{\max(0, S_u - \boldsymbol{S_{umax}})}{\boldsymbol{\Delta t}}$<br>$R_{fl} = R_f$<br>Hillslope:<br>$R_f = (1 - \boldsymbol{W}) \cdot C \cdot P_e$<br>$R_{fl} = R_f * f(T_{lag})$ |
| **Groundwater** | $\frac{\Delta S_s}{\boldsymbol{\Delta t}} = R_{r_{tot}} - R_{c_{tot}} - Q_s$ | $R_r = \boldsymbol{W} \cdot C \cdot P_e$<br>$R_{r_{tot}} = \sum_{HRU} \boldsymbol{p_{HRU}} \cdot R_r$<br>$R_{c_{tot}} = \sum_{HRU} \boldsymbol{p_{HRU}} \cdot R_c$<br>$Q_s = \frac{S_s}{\boldsymbol{K_s}}$ |
| **Total runoff** | $Q_m = Q_s + Q_{f_{tot}}$ | $Q_{f_{tot}} = \sum_{HRU} \boldsymbol{p_{HRU}} \cdot Q_f$ |
| **Supporting literature** | (Gharari et al., 2014;Gao et al., 2014;Euser et al., 2015) | |

https://doi.org/10.5194/hess-2019-346
Preprint. Discussion started: 10 September 2019


245

### 3.3 Parameter selection procedures and model performance evaluation

To evaluate the information content and thus the utility of altimetry data for the selection of feasible model parameter sets, a step-wise procedure as specified in detail below was applied. Note that given data scarcity and the related issues of epistemic uncertainties (Beven and Westerberg, 2011;McMillan and Westerberg, 2015) and
250 equifinality (Beven, 2006;Savenije, 2001) we did not aim to identify the "optimal" parameter set in what is frequently considered a traditional calibration approach. In most hydrological applications the available data have limited strength for rigorous model tests (Clark et al., 2015;Gupta et al., 2008;Jakeman and Hornberger, 1993). Thus, to reduce type II errors of rejecting good parameters when they should have been accepted (Beven, 2010;Hrachowitz and Clark, 2017), we rather attempted to identify and discard the most implausible parameter
255 sets (Freer et al., 1996) that violate our theoretical understanding of the system or that are inconsistent with the available data (Knutti, 2008). This allowed us to iteratively constrain the feasible parameter space and thus the uncertainty around the modelled hydrograph (Hrachowitz et al., 2014). To do so, a Monte-Carlo sampling strategy with uniform prior parameter distributions was applied to generate $5 \cdot 10^4$ model realizations. This random set of solutions was in the following steps used as baseline and iteratively constrained by identifying
260 parameter sets that do not satisfy pre-specified criteria (see below), depending on the data type and source used.

#### 3.3.1 Benchmark: Parameter selection and model performance based on observed discharge data

**Model calibration**

As benchmark, and following a traditional calibration procedure, the model was calibrated with observed daily discharge based on the Nash-Sutcliffe efficiency (Nash and Sutcliffe, 1970) using all complete hydrological
265 years within the time period 2002 to 2016; these are the years starting in the fall of 2004, 2006 and 2008:

$$E_{\mathrm{NS,Q}} = 1 - \frac{\sum_t \left(Q_{\mathrm{mod}}(\mathrm{t}) - Q_{\mathrm{obs}}(t)\right)^2}{\sum_t (Q_{\mathrm{obs}}(\mathrm{t}) - \overline{Q_{\mathrm{obs}}})^2} \quad (1)$$

To limit the solutions to relatively robust representations of the system while allowing for data and model uncertainty (e.g. Beven, 2006;Beven and Westerberg, 2011) only parameter sets that resulted in $E_{NS,Q} \geq 0.6$ were retained as feasible. The hydrological model consisted of 17 free calibration parameters whose uniform prior distributions are given in Table S1 in the supplementary material with associated parameter constrains as
270 summarised in Table S2.

**Model evaluation**

The performance of all model realizations was evaluated post-calibration with respect to discharge using seven additional hydrological signatures (e.g. Sawicz et al., 2011;Euser et al., 2013) to assess the skill of the model to
275 reproduce the overall response of the system and thus the robustness of the selected parameters (Hrachowitz et al., 2014). The signatures included the logarithm of the daily flow time series (hereafter referred to with the subscript logQ), the flow duration curve (FDC), its logarithm (logFDC), the mean seasonal runoff coefficient during dry periods (April - September; RCdry), the mean seasonal runoff coefficient during the wet periods (October - March; RCwet), the autocorrelation function of daily flow (AC) and the rising limb density of the
280 hydrograph (RLD). Detailed explanations of these signatures can be found in Euser et al. (2013) and references therein. As performance measures for the model to reproduce the individual observed signatures the Nash-

https://doi.org/10.5194/hess-2019-346
Preprint. Discussion started: 10 September 2019




Sutcliffe efficiency ($E_{NS,logQ}$, $E_{NS,FDC}$, $E_{NS,logFDC}$, $E_{NS,AC}$; equivalent to Eq.(**1**) and a metric based on the relative error ($E_{R,RCdry}$, $E_{R,RCwet}$, $E_{R,RLD}$) were used (Euser et al., 2013):

$$E_{R,\theta} = 1 - \frac{|\theta_{mod} - \theta_{obs}|}{\theta_{obs}} \quad (2)$$

Where $\theta$ is any of the three signatures evaluated with $E_R$. The signatures where combined, with equal weights, into one objective function, which was formulated based on the Euclidian distance $D_E$ (Schoups et al., 2005) so that a value of 1 indicates a "perfect" model:

$$D_E = 1 - \sqrt{\frac{1}{(N+M)}\left(\sum_n \left(1 - E_{NS,\theta_n}\right)^2 + \sum_m \left(1 - E_{R,\theta_m}\right)^2\right)} \quad (3)$$

Where $\theta$ is a signature, $n$ indicates the signatures evaluated based on the Nash-Sutcliffe efficiency, $m$ indicates the signatures evaluated based on the relative error and N and M are the respective number of signatures used.

### 3.3.2 Parameter selection and model performance based on the seasonal water storage (GRACE)

In a next step we assumed that discharge records in the Luangwa Basin were absent. The starting assumption thus had to be that all model realizations, i.e. all sampled parameter sets, were equally likely to allow feasible representations of the hydrological system. In a stepwise approach, confronting these realizations with different types of data, we sequentially identified and discarded solutions that were least likely to provide meaningful system representations, thereby gradually narrowing down the feasible parameter space.

As altimetry data alone only contain limited information on the river flow volumes, we first identified and discarded solutions that were least likely to preserve observed the seasonal water storage ($S_{tot}$) fluctuations. To do so, the monthly modelled total water storage ($S_{tot,mod} = S_i + S_u + S_f + S_s$) relative to the 2004-2009 time-mean baseline in each grid cell was compared to water storage anomalies as obtained from the GRACE data product (Tang et al., 2017;Fang et al., 2016;Forootan et al., 2019;Khaki and Awange, 2019). In the GRACE product, the same time period was used for the time-mean baseline (Swenson and Wahr, 2006;Swenson, 2012;Landerer and Swenson, 2012).

The model's skill to reproduce the seasonal water storage, i.e. $S_{tot}$, was assessed using the Nash-Sutcliffe efficiency $E_{NS,Stot}$ (Eq. (**1**). Note that $E_{NS,Stot,j}$ was computed at first from the time series of $S_{tot}$ in each grid cell $j$ which were then averaged to obtain $E_{NS,Stot}$. If no additional data were available, a hypothetic modeller relying on $E_{NS,Stot}$ to calibrate a model, may choose only the solution with the highest $E_{NS,Stot}$ or allow for some uncertainty. To mimic this traditional approach but to balance it with a sufficient number of feasible solutions to be kept for the subsequent steps we here identified and discarded the poorest performing 75% of all solutions in terms of $E_{NS,Stot}$ as unfeasible for the subsequent modelling steps.

### 3.3.3 Parameter selection and model performance based on satellite altimetry data

Next, the remaining feasible parameter sets were used to evaluate their potential to also reproduce time series of observed altimetry applying three distinct parameter selection and model evaluation strategies. Assuming again the situation of an ungauged basin (i.e. no time-series of river flow available), we kept for each strategy as feasible the respective 1% best performing parameter sets according to the specific performance metric

https://doi.org/10.5194/hess-2019-346
Preprint. Discussion started: 10 September 2019




associated to that strategy. In a final step, these solutions were then compared for their potential to reproduce actually observed river flow time series.

**Altimetry Strategy 1: Direct comparison of altimetry data to modelled discharge**

Hereafter referred to as with subscript WL, i.e. water level. In the simplest approach, we directly used altimetry data to correlate observed water levels with modelled discharge based on the Spearman rank correlation coefficient ($E_{R,WL}$; Spearman, 1904):

$$E_{\mathrm{R,WL}} = \frac{\mathrm{cov}(r_{\mathrm{Q_{mod}}}, r_{\mathrm{WL_{obs}}})}{\sigma\left(r_{\mathrm{Q_{mod}}}\right) * \sigma(r_{\mathrm{WL_{obs}}})} \quad (4)$$

Where $r_{Q,mod}$ and $r_{WL,obs}$ are the ranks of the modelled discharge and the observed water levels, respectively. This method requires as assumption that the relationship between water level and discharge has to be monotonic. The Spearman rank correlation was applied successfully in previous studies to calibrate a rainfall-runoff model to water level time series (Seibert and Vis, 2016). As there were multiple virtual stations with water level data available in this study, the $E_{R,WL}$ was computed at each location simultaneously. The individual values $E_{R,WL}$ were weighted based on the record length of the corresponding virtual stations and then combined into the Euclidean distance as aggregate metric $D_{E,R,WL}$, equivalent to (**3**.

**Altimetry Strategy 2: Rating curves**

In the second strategy, as successfully applied in previous studies (Getirana and Peters-Lidard, 2013;Jian et al., 2017), model parameters were selected based on the models' ability to reproduce water levels by converting the modelled discharge to water levels, assuming these two are related through a rating curve in the form of a power function (Rantz, 1982):

$$Q = a * (h - h_0)^b \quad (5)$$

Where $h$ is the water level, $h_0$ a reference water level, and $a$ and $b$ are two additional calibration parameters, determining the shape of the function and lumping the combined influences of different river cross-section characteristics, such as geometry or roughness. Note, that here for each virtual station $h_0$ is the elevation that corresponds to the water level of the Google Earth image with the lowest flow available. This strategy is hereafter referred to as with subscript RC, i.e. rating curve. As river-cross sections vary in space, each of the 18 virtual stations would require an individual set of these parameters $a$ and $b$. To limit the number of additional calibration parameters, we here classified the river-cross sections of the 18 virtual stations into 4 classes (Figure 1A and Figure 3). For cross-sections within each class, i.e. geometrically similar, the same values for $a$ and $b$ were used, resulting in 4 sets of $a$ and $b$ and thus a total of 8 additional calibration parameters. The river cross-sections were extracted from global high-resolution terrain data available on Google Earth (see Section 2.1.4). The modelled river water levels were evaluated against the observed water levels at each virtual station using the Nash-Sutcliffe efficiency $E_{NS,RC}$ (equivalent to Eq. (**1**), weighted based on the record length of the corresponding virtual stations and then combined into the Euclidean distance $D_{E,NS,RC}$ as an aggregated performance metric (Eq. (**3**).

https://doi.org/10.5194/hess-2019-346
Preprint. Discussion started: 10 September 2019


Hydrology and Earth System Sciences
Discussions
Open Access
EGU

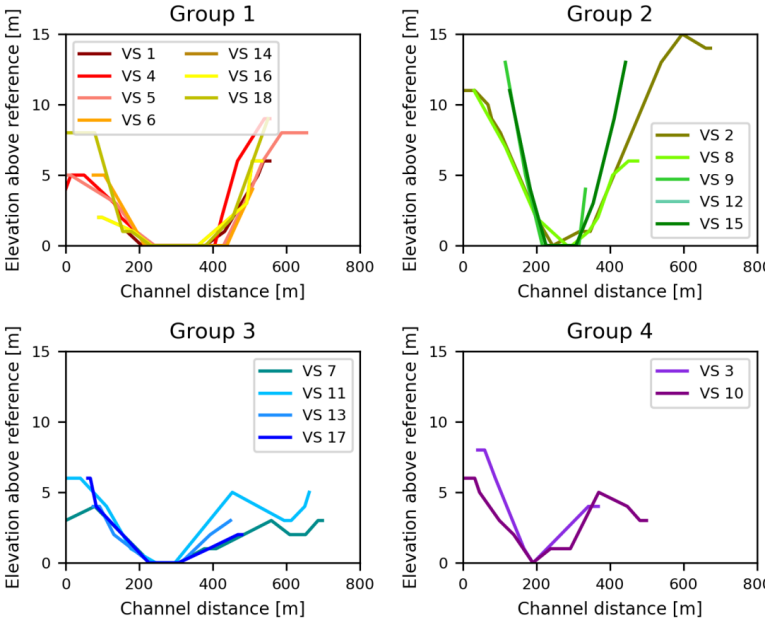


**Figure 3: River profiles at 18 virtual stations (VS) divided into four groups. The reference level is equal to the lowest water level in the river profile for each location separately.**

355

**Altimetry Strategy 3: Strickler-Manning equation**

As third strategy, we converted the modelled discharge to river water levels using the Strickler-Manning equation (Manning, 1891):

$$Q = k * i^{\frac{1}{2}} * A * R^{\frac{2}{3}} \tag{6}$$

Where $k$ is a roughness parameter, here treated as free calibration parameter and assumed constant for all virtual
360 stations, $i$ is the mean channel slope, here over a distance of 10 km, while $A$ and $R$ are the river cross-section area and hydraulic radius. Assuming trapezoidal cross-sections (see Figure 4 as illustrative example), $A$ and $R$ were calculated for each cross section according to:

$$A = B * d + \frac{1}{2} * d^2 * (i_1 + i_2) \tag{7}$$

$$R = \frac{A}{B + d * \left( (1 + i_1^2)^{\frac{1}{2}} + (1 + i_2^2)^{\frac{1}{2}} \right)} \tag{8}$$

$$d = h - h_0 \tag{9}$$

Where $B$ is the assumed river bed width, $i_1$ and $i_2$ are the river bank slopes, $d$ the water depth, $h$ the water level and $h_0$ the reference water level, here assumed to be the lowest observed river water level to limit the number of
365 calibration parameters. In contrast to previous studies that use a similar approach but relied on locally observed river-cross sections (Michailovsky et al., 2012;Hulsman et al., 2018;Liu et al., 2015), here both, the river bed geometries (Figure 3) at and the channel slopes upstream of the 18 virtual stations were computed using high-resolution terrain data retrieved from Google Earth (see Section 2.1.4); similar data sources were already used in previous studies to extract the river geometry (e.g. Michailovsky et al., 2012;Pramanik et al., 2010;Gichamo et

https://doi.org/10.5194/hess-2019-346
Preprint. Discussion started: 10 September 2019




al., 2012). The reader is referred to Table S3 in the supplementary material for the values of the variables for each virtual station. This strategy is hereafter referred to as with subscript SM, i.e. Strickler-Manning.

Equivalent to above, the modelled river water levels were then evaluated against the observed water levels at each virtual station using the Nash-Sutcliffe efficiency $E_{NS,SM}$ (equivalent to Eq. (**1**), weighted based on the record length of the corresponding virtual stations and then combined into the Euclidean distance $D_{E,NS,SM}$ as an aggregated performance metric (Eq. (**3**).

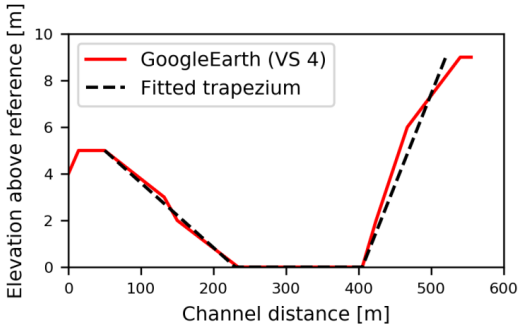


**Figure 4: Example of approximating a trapezoidal cross-section (black) into the Google Earth based cross-section data (red) for virtual station "VS 4" (see also Figure 1A and Figure 3). The reference level is equal to the lowest water level in the river profile.**

### 3.3.4 Parameter selection and model performance based on daily river water level at the basin outlet

In-situ measurements were available though at the Great East Road Bridge gauging station, the catchment outlet. As shown in Figure 5, the Google Earth based above-water cross-section at the basin outlet corresponded in general well to the field survey considering that satellite images have limited spatial resolution. However, the in-situ measurement also illustrated the relevance of the submerged part of the channel cross-section at that location on the day the image was taken (June 2nd 2008). To assess the influence of the cross-section accuracy, model parameter sets were selected based on the models' ability to reproduce daily stream levels at the Great East Road Bridge gauging station, i.e. the basin outlet.

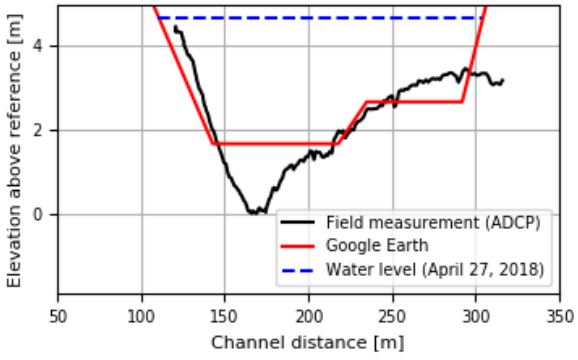


**Figure 5: River cross-section at Luangwa Bridge obtained from Google Earth and detailed field survey including the river water level on June 2nd 2008. Field measurements were done with an Acoustic Doppler Current Profiler (ADCP) on April 27th 2018 at the coordinates 30° 13' E and 15° 00' S; the satellite image was taken on June 2nd 2008. The reference level is equal to the lowest elevation level measured with the ADCP.**

https://doi.org/10.5194/hess-2019-346
Preprint. Discussion started: 10 September 2019


Hydrology and Earth System Sciences
Discussions

**Water level Strategy 1: River geometry information extracted from Google Earth**

First, cross-section information was extracted from global high-resolution terrain data available on Google Earth (subscript GE) and used with the Strickler-Manning equation (Eq. (**6**) to convert the modelled discharge to water levels. This was combined with GRACE observations to restrict the parameter space in an equivalent way as in Section 3.3.3. The model performance with respect to river water levels was calculated with the Nash-Sutcliffe efficiency $E_{NS,SM,GE}$ (Eq. (**1**).

**Water level Strategy 2: River geometry information obtained from a detailed field survey**

Second, cross-section information obtained from a detailed field survey with an ADCP (subscript ADCP) was used with the Strickler-Manning equation (Eq. (**6**) to convert the modelled discharge to water levels. This was combined with GRACE observations to restrict the parameter space in an equivalent way as in Section 3.3.3. The model performance with respect to river water levels was calculated with the Nash-Sutcliffe efficiency $E_{NS,SM,ADCP}$ (Eq. (**1**).

## 4 Results and discussion

### 4.1 Parameter selection and model performance

The complete set of all model realizations unsurprisingly results in a wide range of model solutions (Figure 6A), with $E_{NS,Q}$ ranging from -6.4 to 0.78 and with the combined performance metric of all signatures $D_E$ ranging from -334 to 0.79 (Figure 7). Although containing relatively good solutions, this full set of all realizations clearly also contained many parameter sets that considerably over- and/or underestimate flows.

https://doi.org/10.5194/hess-2019-346
Preprint. Discussion started: 10 September 2019


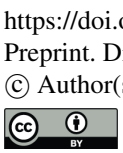

Hydrology and Earth System Sciences
Discussions

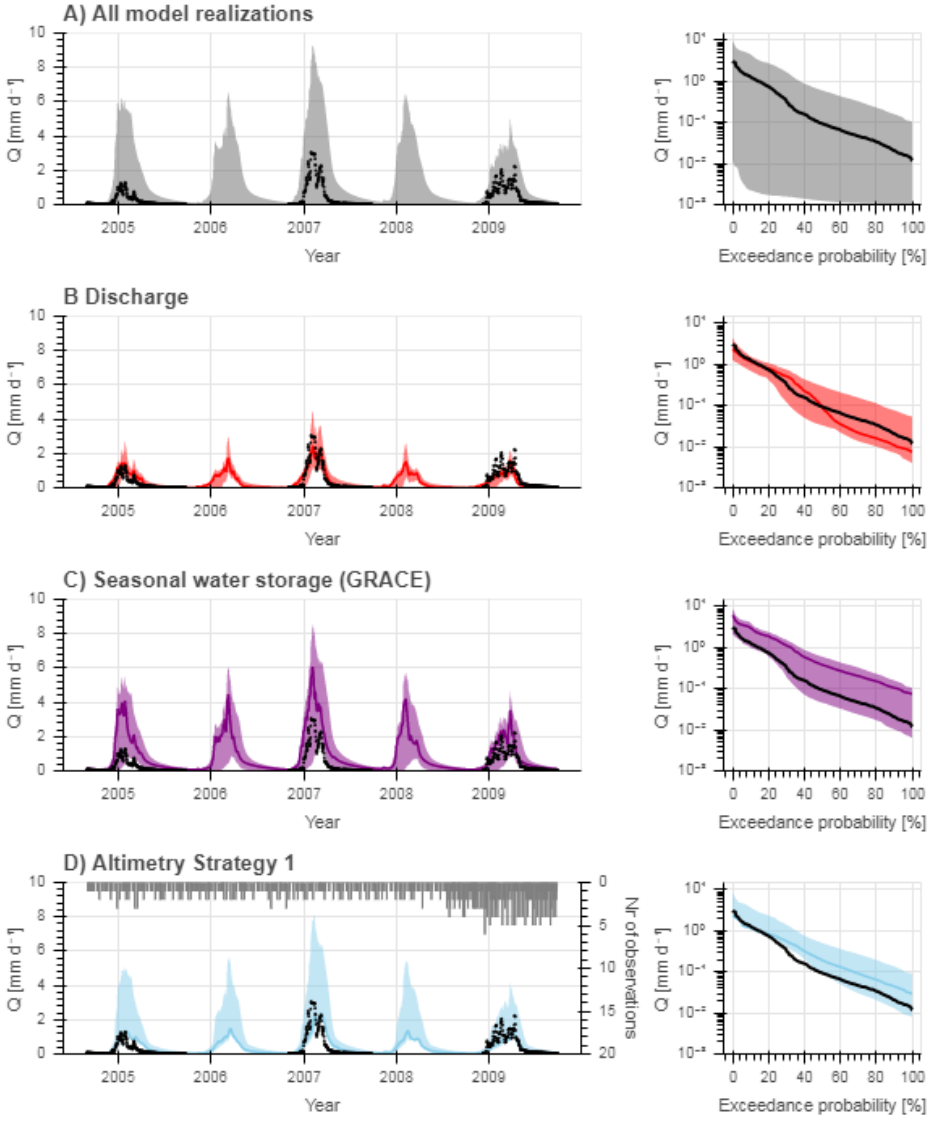


415

**Figure 6: Range of model solutions. The left panel shows the hydrograph and the right panel the flow duration curve of the recorded (black) and modelled discharge: the line indicates the solution with the highest calibration objective function ($E_{NS}$ or $D_E$) and the shaded area the envelope of the solutions retained as feasible. A) All model solutions**
420 **included; solutions retained as feasible based on B) discharge (i.e. "traditional calibration"; $E_{NS,Q}$), C) GRACE ($E_{NS,Stot}$), and D) Altimetry Strategy 1 only ($D_{E,R,WL}$).The grey bars in the left subplot D indicate the number of altimetry observations available for each day.**

https://doi.org/10.5194/hess-2019-346
Preprint. Discussion started: 10 September 2019


Hydrology and Earth System Sciences
Discussions
Open Access
EGU

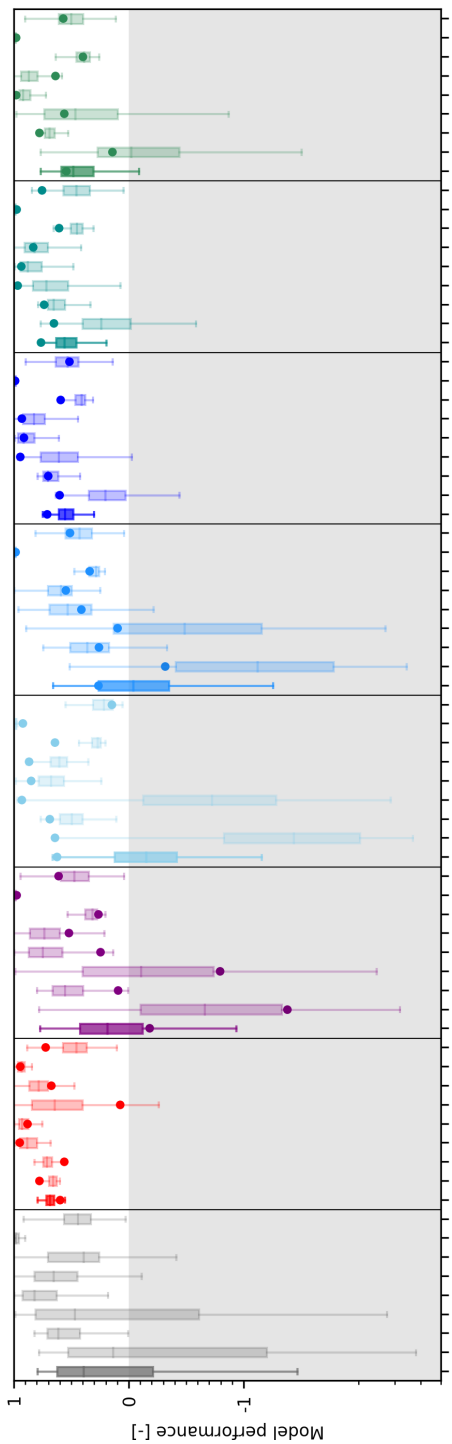


**Figure 7: Comparison of different data sources to identify feasible parameter sets. Data sources applied: 1) All random parameters (no data), 2) Discharge, 3) GRACE, 4) Altimetry data combined with GRACE (Altimetry Strategy 1), 5) Altimetry data using the rating curves combined with GRACE (Altimetry Strategy 2), and 6) Altimetry data using the Strickler – Manning equation combined with GRACE (Altimetry Strategy 3), and 7) Daily river water level combined with GRACE using the Strickler – Manning equation and cross-section information retrieved from Google Earth (Water level Strategy 1), or 8) obtained from a detailed field survey with an Acoustic Doppler Current Profiler (ADCP, Water level Strategy 2). The boxplots visualise the spread in the overall model performance $D_E$ with respect to discharge and the following individual signatures: a) daily discharge ($E_{NS,Q}$), b) its logarithm ($E_{NS,logQ}$), c) flow duration curve ($E_{NS,FDC}$), d) its logarithm ($E_{NS,logFDC}$), e) average runoff coefficient during the dry season ($E_{R,RCdry}$), f) average seasonal runoff coefficient during the wet season ($E_{R,RCwet}$), g) autocorrelation function ($E_{NS,AC}$), and h) rising limb density ($E_{R,RLD}$). The dots visualise the model performance when selecting the parameter set with the highest model efficiency according to each parameter identification strategy.**

https://doi.org/10.5194/hess-2019-346
Preprint. Discussion started: 10 September 2019


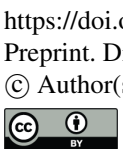

Hydrology and Earth System Sciences
Discussions
Open Access
EGU

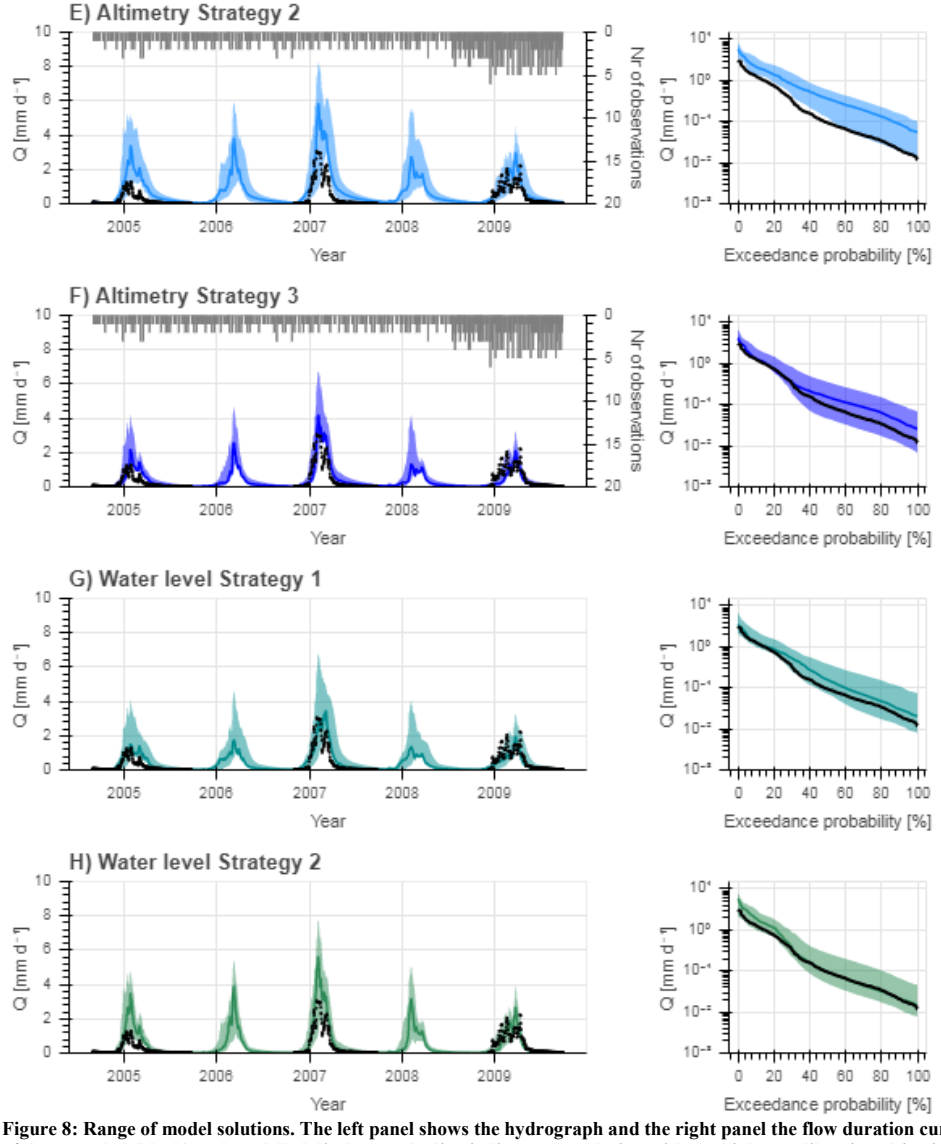


**Figure 8: Range of model solutions. The left panel shows the hydrograph and the right panel the flow duration curve of the recorded (black) and modelled discharge: the line indicates the solution with the highest calibration objective function ($E_{NS}$ or $D_E$) and the shaded area the envelope of the solutions retained as feasible. Solutions retained as feasible based on E) Altimetry Strategy 2 using rating curves for the discharge – water level conversion ($D_{E,NS,RC}$), F) Altimetry Strategy 3 using the Strickler-Manning equation for the discharge – water level conversion ($D_{E,NS,SM}$), and G) Daily in-situ water level using the Strickler Manning equation for the discharge – water level conversion with cross-section information retrieved from Google Earth (Water level strategy 1; $E_{NS,SM,GE}$) or H) obtained from a detailed field survey with an Acoustic Doppler Current Profiler (ADCP; Water level strategy 2; $E_{NS,SM,ADCP}$). The grey bars in the left subplots E and F indicate the number of altimetry observations available for each day.**

https://doi.org/10.5194/hess-2019-346
Preprint. Discussion started: 10 September 2019


Hydrology and Earth System Sciences
Discussions
Open Access
EGU

#### 4.1.1 Benchmark: Parameter selection and model performance based on observed discharge data

As benchmark, to assess which range of feasible parameter sets and solutions would have been obtained from a traditional model calibration approach, the model was calibrated with the available observed discharge data. In other words, only the sub-set of solutions from the above complete set of all model realizations that did satisfy the previously defined criterion (see Section 3.3.1), were retained as feasible. As shown in Figure 6B, this parameter selection and calibration strategy results in a reasonable model performance, in which the seasonal but also the daily flow dynamics and magnitudes are in general well captured. For some years, a number of solutions overestimate flows in the wet season and underestimate flows during the dry season, when the river becomes a small meandering stream with almost annual morphological changes which is difficult to meaningfully observe. The best performing solution has a calibration objective function $E_{NS,Q,opt}$ = 0.78 (5/95$^{th}$ percentiles of all feasible solutions $E_{NS,Q,5/95}$ = 0.61 – 0.75; Figure 7 and Table 4). For the post-calibration evaluation of all retained solutions, it was observed that most signatures are well reproduced by the majority of solutions, except for the dry season runoff coefficient ($RC_{dry}$; Figure 7). This resulted in aggregated model performances, combining all signatures, of $D_{E,5/95}$ = 0.55 – 0.76 with the above identified best performing solution (i.e. $E_{NS,Q,opt}$) reaching a value of $D_{E,opt}$ = 0.60.

**Table 4: Summary of the model results: elimination of unfeasible parameter sets and detection of optimal parameter set according to each parameter identification strategy including the corresponding model performance range ($E_{NS,Q}$, $D_E$) indicating the model's skill to reproduce the discharge during the benchmark time period. For each strategy, the model efficiency for the optimal parameter set is summarised together with the corresponding performance metrics with respect to discharge ($E_{NS,Q,opt}$, $D_{E,opt}$); for all parameter sets retained as feasible, the maximum ($E_{NS,Q,max}$, $D_{E,max}$) and 5/95 percentiles ($E_{NS,Q,5/95}$, $D_{E,5/95}$) of all performance metrics with respect to discharge are summarised. Data sources used for the parameter set selection: 1) All parameter sets (no data), 2) Discharge, 3) GRACE, 4) Altimetry combined with GRACE (Altimetry Strategy 1), 5) Altimetry data using rating curves combined with GRACE (Altimetry Strategy 2), 6) Altimetry data using the Strickler – Manning equation combined with GRACE (Altimetry Strategy 3), and 7) Daily river water level combined with GRACE using the Strickler – Manning equation and cross-section information retrieved from Google Earth (Water level Strategy 1), or 8) obtained from a detailed field survey with an Acoustic Doppler Current Profiler (ADCP, Water level Strategy 2).**

| | Optimal parameter set | | Feasible parameter sets | |
|---|---|---|---|---|
| | **Model efficiency** | **$E_{NS,Q,opt}$ ($D_{E,opt}$)** | **$E_{NS,Q,max}$ ($E_{NS,Q,5/95}$)** | **$D_{E,max}$ ($D_{E,5/95}$)** |
| **1) All parameters sets** | - | - | 0.78 (-3.8 – 0.68) | 0.79 (-1.4 – 0.71) |
| **2) Discharge** | $E_{NS,Q,opt}$ = 0.78 | 0.78 (0.60) | 0.78 (0.61 – 0.75) | 0.79 (0.55 – 0.76) |
| **3) Seasonal water storage (GRACE)** | $E_{NS,Stot,opt}$ = 0.56 | -1.4 (-0.18) | 0.78 (-2.3 – 0.38) | 0.77 (-0.58 – 0.62) |
| **4) Altimetry Strategy 1: Compare altimetry to discharge** | $D_{E,R,WL,opt}$ = 0.76 | 0.65 (0.63) | 0.65 (-2.9 – 0.10) | 0.66 (-0.83 – 0.50) |
| **5) Altimetry Strategy 2: Rating curves** | $D_{E,NS,RC,opt}$ = -0.50 | -0.31 (0.27) | 0.51 (-2.6 – 0.25) | 0.66 (-0.72 – 0.56) |
| **6) Altimetry Strategy 3: Strickler-Manning equation** | $D_{E,NS,SM,opt}$ = -1.4 | 0.60 (0.71) | 0.63 (-0.31 – 0.50) | 0.75 (0.36 – 0.67) |
| **7) Water level Strategy 1: satellite based cross-section** | $E_{NS,SM,GE,opt}$ = -1.8 | 0.65 (0.77) | 0.77 (-0.48 – 0.60) | 0.77 (0.28 – 0.70) |
| **8) Water level Strategy 2: in-situ cross-section** | $E_{NS,SM,ADCP,opt}$ = 0.79 | 0.14 (0.55) | 0.77 (-1.1 – 0.50) | 0.77 (0.03 – 0.67) |

#### 4.1.2 Parameter selection and model performance based on the seasonal water storage (GRACE)

Starting from the set of all model realizations (Figures 6A and 7), and assuming no discharge observations are available, we then identified and discarded parameter sets as unfeasible when they did not meet the previously

https://doi.org/10.5194/hess-2019-346
Preprint. Discussion started: 10 September 2019




defined criteria to reproduce the seasonal water storage ($E_{NS,Stot}$; see Section 3.3.2). The sub-set of solutions retained as feasible resulted in a significant reduction in the uncertainty around the modelled variables, which is illustrated by the narrower 5/95$^{th}$ percentiles of the solutions compared to the set of all realizations, as shown in Figure 6C. The feasible solutions with respect to the GRACE reached $E_{NS,Stot,opt}$ = 0.56 ($E_{NS,Stot,5/95}$ = 0.45 – 0.52) (Figure 7, Table 4). These parameter sets were then used to evaluate the model for the years 2004, 2006, 2008 used in the benchmark case. While the flow dynamics are captured relatively well, many of the retained solutions considerably overestimated flows across all seasons (Figure 6C). The parameter set associated with the best performing model with respect to GRACE ($E_{NS,Stot,opt}$) resulted for the benchmark period in a $E_{NS,Q}$ = -1.4 ($E_{NS,Q,5/95}$ = -2.3 – 0.38) and the corresponding $D_{E,opt}$ = -0.18 ($D_{E,5/95}$ = -0.58 – 0.62) with respect to discharge (Figure 7, Table 4). As illustrated in Figure 7 and Figure 6C, many parameter sets that resulted in implausible representations of the seasonal signals were eliminated. However, as also indicated by the rather modest values of $E_{NS,Q}$ and $D_E$ with respect to discharge, the data source used here obviously contained only limited information to avoid the over predictions of flow during all wet seasons.

#### 4.1.3 Parameter selection and model performance based on satellite altimetry data

After having identified feasible parameter sets based on the seasonal water storage, additional unfeasible parameter sets were eliminated using altimetry data with three different strategies. In all three cases, the best 5% of all feasible parameter sets were selected; this resulted in 1% of all parameter sets.

**Altimetry Strategy 1: Directly compare altimetry data to modelled discharge**

In a first approach, the altimetry data were directly compared to the modelled discharge using the Spearman rank correlation coefficient. As shown in Figure 6D, this resulted in an overestimation of in particular intermediate and low flows. The feasible solutions reached an optimum of $D_{E,R,WL,opt}$ = 0.76 ($D_{E,R,WL,5/95}$ = 0.74 – 0.75) with respect to altimetry observations. Focusing on the model's skill to reproduce the observed discharge using these feasible parameter sets for the benchmark period, the parameter set associated with the best performing model with respect to altimetry ($D_{E,R,WL,opt}$) resulted in a $E_{NS,Q}$ = 0.65 ($E_{NS,Q,5/95}$ = -2.9 – 0.10) and $D_E$ = 0.63 ($D_{E,5/95}$ = -0.83 – 0.50) with respect to discharge (Figure 7, Table 4). While the optimum model performance with respect to discharge was similar to the benchmark, the very wide range in the 5/95$^{th}$ percentiles of the solutions indicated that this strategy has only limited potential to identify implausible parameter sets.

**Altimetry Strategy 2: Rating curves**

In a second approach, altimetry data were compared to the modelled stream water levels by converting the modelled discharge to water levels, based on rating curves. This also resulted in an overestimation of the flows (Figure 8E). The feasible solutions reached an optimum of $D_{E,NS,RC,opt}$ = -0.50 ($D_{E,NS,RC,5/95}$ = -1.0 – -0.77) with respect to altimetry observations. Focusing on the model's skill to reproduce the discharge using these parameter sets for the benchmark period, the parameter set associated with the best performing model with respect to altimetry ($D_{E,NS,RC,opt}$) resulted in $E_{NS,Q}$ = -0.31 ($E_{NS,Q,5/95}$ = -2.6 – 0.25) and $D_E$ = 0.27 ($D_{E,5/95}$ = -0.72 – 0.56) with respect to discharge (Figure 7, Table 4). The optimum model performance with respect to discharge was worse compared to the benchmark, and the wide range in the 5/95$^{th}$ percentiles of the solutions indicated this strategy poorly identified the feasible parameter sets.

https://doi.org/10.5194/hess-2019-346
Preprint. Discussion started: 10 September 2019




515

**Altimetry Strategy 3: Strickler-Manning equation**

In a third approach, the altimetry data were compared to modelled stream water levels by converting the modelled discharge to water levels using the Strickler-Manning equation. This resulted in improved flow predictions compared to the other two strategies using altimetry data (Figure 8F). Even though the feasible
520 solutions exhibit a very poor ability to reproduce the altimetry data, with an optimum of $D_{E,NS,SM,opt}$ = -1.4 ($D_{E,NS,SM,5/95}$ = -3.8 – -1.8), the model's skill to reproduce the discharge for the benchmark period using these parameter sets, significantly increased compared to the two alternative strategies. The parameter set associated with the best performing model with respect to altimetry ($D_{E,NS,SM,opt}$) resulted in $E_{NS,Q}$ = 0.60 ($E_{NS,Q,5/95}$= -0.31 – 0.50) and $D_E$ = 0.71 ($D_{E,5/95}$ = 0.36 – 0.67) with respect to discharge (Figure 7, Table 4). While the optimum
525 model performance with respect to discharge was worse compared to the benchmark, the 5/95$^{th}$ percentiles of the solutions were significantly constrained by the removal of many implausible parameter sets. This indicated that, although the model performance with respect to altimetry observations was low, this strategy contains valuable information to considerably constrain the feasible solution space.

**4.1.4 Parameter selection and model performance based on daily river water level at the basin outlet**

530 In this approach, daily river water level observations at the basin outlet only was compared to modelled stream levels by converting the modelled discharge to water levels with the Strickler-Manning equation using cross-section information 1) extracted from global high-resolution terrain data available on Google Earth (subscript GE) and 2) obtained from a detailed field survey (subscript ADCP).

535 **Water level Strategy 1: River geometry information extracted from Google Earth**

First, using cross-section information extracted from Google Earth resulted in a poor simulation of the river water level (Figure 9A) with an optimal objective function value with respect to river water levels of $E_{NS,SM,GE,opt}$ = -1.8 ($E_{NS,SM,GE,5/95}$ = -6.8 – -3.1). Focusing on the model's skill to reproduce the discharge using these feasible parameter sets for the benchmark period, the parameter set associated with the best performing model with
540 respect to river water levels ($E_{NS,SM,GE,opt}$) resulted in $E_{NS,Q,GE}$ = 0.65 ($E_{NS,Q,5/95,GE}$ = -0.48 – 0.60) and $D_{E,GE}$ = 0.77 ($D_{E,GE,5/95}$ = 0.28 – 0.70) with respect to discharge (Figure 7, Table 4). As shown in Figure 8G, the discharge was overestimated in particular during intermediate and low flows.

**Water level Strategy 2: River geometry information obtained from a detailed field survey**

545 Second, using cross-section information obtained from a detailed field survey resulted in improved river water level simulations (compare Figure 9A and B) with an optimal objective function value with respect to river water levels of $E_{NS,SM,ADCP,opt}$ = 0.79 ($E_{NS,SM,ADCP,5/95}$ = 0.60 – 0.74). The parameter set associated with the best performing model with respect to river water levels ($E_{NS,SM,ADCP,opt}$) resulted in $E_{NS,Q,ADCP}$ = 0.14 ($E_{NS,Q,5/95,ADCP}$ = -1.1 – 0.50) and in $D_{E,ADCP}$ = 0.55 ($D_{E,ADCP,5/95}$ = 0.03 – 0.67) with respect to discharge (Figure 7, Table 4).
550 Compared to using river geometry information extracted from Google Earth (Water level Strategy 1), the overall model performance with respect to discharge did not increase since the parameter space was already restricted using GRACE data. However, the modelled flow duration curve during intermediate and low flows (compare Figure 8G with H) and rating curve (Figure 10) improved significantly when using more accurate geometry

https://doi.org/10.5194/hess-2019-346
Preprint. Discussion started: 10 September 2019


Hydrology and Earth System Sciences
Discussions

information obtained from a detailed field survey covering the cross-section that is submerged most of the year which is thus unlikely to be captured by satellite based observations. Note, that the in-situ cross-section information was limited to the submerged part during the time of measurement; the remaining part (water levels > 5 m) was extrapolated which is likely to explain the larger discrepancies during high flows visible in the flow duration curve (Figure 8H).

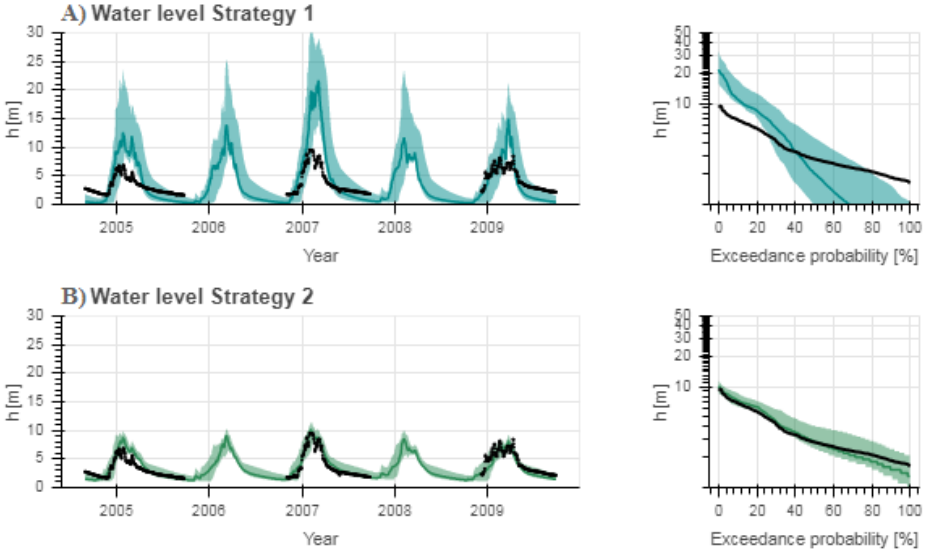


**Figure 9: Range of model solutions. The left panel shows the hydrograph and the right panel the flow duration curve of the recorded (black) and modelled discharge: the line indicates the solution with the highest calibration objective function ($E_{NS}$) and the shaded area the envelope of the solutions retained as feasible. Solutions were retained as feasible based on daily water level time series at the basin outlet using the Strickler-Manning equation for the discharge – water level conversion; the cross-section was A) extracted from Google Earth (Water level Strategy 1), or B) obtained from a detailed field survey with an Acoustic Doppler Current Profiler (ADCP, Water level Strategy 2).**

https://doi.org/10.5194/hess-2019-346
Preprint. Discussion started: 10 September 2019


Hydrology and Earth System Sciences
Discussions

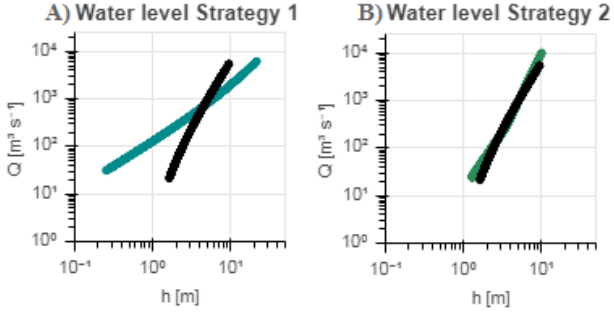


**Figure 10: Discharge - water level graphs for the recorded (black) and modelled discharge and stream levels with the optimal model performance ($E_{NS}$) using the Strickler Manning equation for the discharge – stream level conversion with cross-section information A) extracted from Google Earth (Water level Strategy 1), or B) obtained from a detailed field survey with an Acoustic Doppler Current Profiler (ADCP, Water level Strategy 2).**

### 4.2 Number of virtual stations used for model calibration and evaluation

In this study, altimetry data was available at 18 virtual stations. However, would the model performance change if more or less virtual stations were used? For this purpose, $n$ random stations were selected for model calibration; the remaining stations were used for cross-validation (KlemeŠ, 1986;Gharari et al., 2013;Garavaglia et al., 2017). This was repeated to cover all combinations of $n$ stations and for $n$ = 1, 2 … 17. When applying Strategy 3 using altimetry data with the Strickler-Manning equation, this analysis revealed that when increasing the number of calibration stations, the model calibration performance $D_{E,NS,SM}$ gradually decreased, but the ability to meaningfully reproduce the remaining observations which were not used for calibration increased significantly (Figure 11). Similar results were obtained for Strategies 1 and 2 (compare Figure 11 with Supplementary Figures S3 and S4). This provides evidence that in spite of reduced calibration performance, the simultaneous use of multiple virtual stations can contribute towards more plausible selections of model parameter sets and thus increase the model realism.

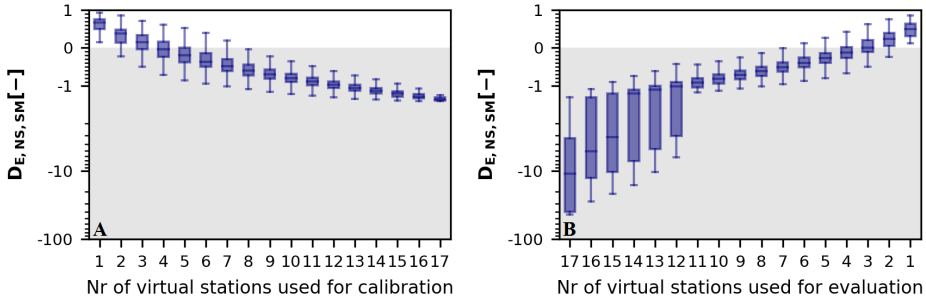


**Figure 11: Influence of the number of virtual stations used for A) model calibration and B) evaluation on the model performance $D_{E,NS,SM}$ applying Altimetry Strategy 3.**

### 4.3 Limitations

In the absence of discharge data for hydrological model calibration as commonly the case in poorly or ungauged regions, freely and globally available remotely sensed stream water levels could provide the opportunity to fill this gap as illustrated in this study, as well as in previous studies (e.g. Michailovsky and Bauer-Gottwein,

https://doi.org/10.5194/hess-2019-346
Preprint. Discussion started: 10 September 2019


Hydrology and Earth System Sciences
Discussions

2014;Pereira-Cardenal et al., 2011;Sun et al., 2012). However, there are several limitations to the approach proposed in this study using altimetry for model calibration.

First, river altimetry data are prone to large uncertainties which increase for smaller river widths (Sulistioadi et al., 2015;Biancamaria et al., 2017). For example, the RMSE of the altimetry data was about 0.6 m to 0.9 m in the Po river (Europe) using Envisat (Tarpanelli et al., 2013;Tourian et al., 2016); in the Ogooué river (Africa) about 0.2 m to 0.5 m using SARAL and Envisat (Bogning et al., 2018); and in the Mekong river (Asia) about 0.44 m to 0.65 m using Envisat (Birkinshaw et al., 2010). Unfortunately, this uncertainty could not be estimated for the virtual stations used in this study due to data limitations. However, in previous studies in the Zambezi Basin, the RMSE relative to in-situ stream levels ranged between 0.32 m and 0.72 m using Envisat (Michailovsky et al., 2012) .

Besides altimetry, data uncertainties in the precipitation, temperature used to estimate the potential evaporation and GRACE based total storage anomalies should not be ignored. Large uncertainties in the forcing data (precipitation and temperature) with respect to the spatial-temporal variations, could compromise comparison results between modelled river water levels and altimetry within the basin since it has a low temporal resolution (10 or 35 days). Also, bias in the forcing data affects storage calculations and hence also the identification of feasible parameter sets based on GRACE; this could explain why the flows were frequently overestimated when using GRACE only. There are also data uncertainties in the cross-sections retrieved from Google Earth due to its limited spatial resolution, but more importantly since no information is available below the water surface.

Uncertainties were not only introduced by the data, but also as a result of assumptions and simplifications. First, the reference level $h_0$ was assumed to be equal to the lowest river water level observed to limit the number of calibration parameters (Altimetry Strategy 2 and 3, Water level Strategy 1 and 2). In reality however, this could be slightly different due to the increasing uncertainties during low flows when the river becomes more narrow and due to the low temporal resolution possibly missing the lowest water level. Second, the roughness was assumed to be constant over the entire cross-section and for all virtual stations throughout the basin which affects the discharge - water level conversion and therefore also the model efficiency (Altimetry Strategy 3). Third, all 18 virtual stations were grouped based on their cross-section similarity to limit the number of calibration parameters (Altimetry Strategy 2), but differences within each group remain which could influence the discharge-water level conversion and therefore also the model efficiency; hence, there is a trade-off in allowing differences between virtual stations and introducing more calibration parameters. Fourth, the assumption of a constant flow velocity in space and time affects the timing of the flow influencing the comparison between model results and altimetry observations (all strategies).

Another limitation is the missing flow volume information when directly using (satellite based) river water levels for model calibration, using, for example, the Spearman Rank Correlations as model performance metric (Altimetry Strategy 1; Seibert and Vis, 2016). This resulted here in an overestimation of intermediate and low flows due to the non-linear relation between stream levels and flows.

In contrast, when converting the discharge to stream water levels, flow volume information was included at the cost of introducing additional uncertainties. Converting modelled discharge to stream levels using rating curves introduced additional free calibration parameters (Altimetry Strategy 2), thereby increasing the degrees-of-freedom and thus the potential for parameter equifinality in the model (Beven, 2006). This is illustrated here by

https://doi.org/10.5194/hess-2019-346
Preprint. Discussion started: 10 September 2019


the eight calibration parameters introduced for Altimetry Strategy 2, which were poorly defined as also observed in previous studies (e.g. Sun et al., 2012;Sikorska and Renard, 2017).

However, converting modelled discharge to stream water levels with the Strickler-Manning equation (Altimetry Strategy 3) required, besides the introduction of a single calibration parameter (roughness), the estimation of the channel cross-section and river gradient. Clearly, both of these variables are subject to uncertainties, which in this study include the limited spatial resolution of the satellite images available on Google Earth.

### 4.4 Comparison with previous studies

Previous studies have successfully used river altimetry data to calibrate and evaluate rainfall-runoff models using a few virtual stations (Sun et al., 2012;Getirana, 2010;Getirana et al., 2010;Liu et al., 2015). In these studies, the modelled discharge was converted to stream levels by means of a hydraulic model or empirical relations. Our results support several previous findings and added a number of new ones.

Similar to previous studies, the rainfall-runoff model reproduced river flow relatively well when calibrating on remotely sensed stream water levels preferably at several virtual stations simultaneously, but discharge based calibration results performed significantly better (Getirana, 2010). Thus, while river altimetry data cannot fully substitute discharge observations, they at least provide an alternative data source that holds some informative value where no reliable discharge data are available. In addition, our results suggest that in spite of the typically limited temporal resolution of altimetry observations, these data, when using multiple virtual stations simultaneously, provide enough information to select meaningful model parameter sets (Seibert and Beven, 2009;Getirana, 2010). Similar to previous studies we obtained comparably insensitive posterior parameter distributions when using rating curves to convert discharge to stream water levels for stream water level based calibrations. This indicated that the calibration parameters associated with the rating curves introduced with this method were not well-defined, thereby leading to increased model uncertainties (Sun et al., 2012;Sikorska and Renard, 2017).

In contrast to previous studies, altimetry data originated from five different satellite missions rather than a single one. As a result, altimetry data was available at 18 locations for the time period 2002 to 2016. This gave the opportunity to analyse the effect of combining different numbers of stations for calibration and evaluation. This study illustrated that better predictions can be achieved when using more virtual stations for calibration. Furthermore, this study demonstrated that in particular the combination of altimetry with information on river geometry (cross section, gradient) proved beneficial for the selection of feasible parameter sets within relatively narrow bounds comparable to the benchmark using discharge. When using more accurate cross-section information obtained from a detailed field survey rather than Google Earth based estimates, improved the water level simulations, modelled rating curve and discharge simulations during intermediate and low flows significantly for which on-site cross-section data was available. That is why it is recommended to acquire accurate cross-section information on locations concurring with altimetry overpasses (not done is this study).

In the Zambezi river basin, altimetry data has been used in previous studies for hydrological modelling (Michailovsky and Bauer-Gottwein, 2014;Michailovsky et al., 2012). These studies used the altimetry data from the Envisat satellite in an assimilation procedure to update states in a Muskingum routing scheme. Including the altimetry data improved the model performance; especially when the model initially performed poorly due to high model complexity or input data uncertainties.

https://doi.org/10.5194/hess-2019-346
Preprint. Discussion started: 10 September 2019


Hydrology and Earth System Sciences
Discussions

## 5 Summary and conclusion

This study investigated the potential value of river altimetry observations from multiple satellite missions to identify feasible parameters for a hydrological model of the semi-arid and poorly gauged Luangwa River Basin. A distributed process-based rainfall-runoff model with sub-grid process heterogeneity was developed on a daily timescale for the time period 2002 to 2016. Various parameter identification strategies were implemented step-wise to assess the potential of satellite altimetry data for model calibration. As benchmark, when identifying parameter sets with the traditional model calibration strategy using discharge data, the model was able to simulate the flows relatively well ($E_{NS,Q}$ = 0.78, $E_{NS,Q,5/95}$ = 0.61 – 0.75). When assuming no discharge observations are available, the feasible parameter sets were restricted with GRACE data only resulting in an optimum of $E_{NS,Q}$ = -1.4 ($E_{NS,Q,5/95}$ = -2.3 – 0.38) with respect to discharge. Combining GRACE with altimetry data only from 18 virtual stations focusing on the water level dynamics resulted in frequently overestimated flows and poorly identified feasible parameter sets (Altimetry Strategy 1, $E_{NS,Q,5/95}$ = -2.9 – 0.10). This was also the case when converting modelled discharge to water levels using rating curves (Altimetry Strategy 2, $E_{NS,Q,5/95}$ = -2.6 – 0.25). The identification of the feasible parameter sets improved when including river geometry information, more specifically cross-section and river gradient extracted from Google Earth, in the discharge-water level conversion using the Strickler-Manning equation (Altimetry Strategy 3, $E_{NS,Q}$ = 0.60, $E_{NS,Q,5/95}$ = -0.31 – 0.50). Moreover, it was shown that more accurate cross-section data improved the water level simulations, modelled rating curve and discharge simulations during intermediate and low flows for which on-site cross-section information was available; the Nash-Sutcliffe efficiency with respect to river water levels increased from $E_{NS,SM,GE}$ = -1.8 ($E_{NS,SM,GE,5/95}$ = -6.8 – -3.1) using river geometry information extracted from Google Earth (Water level Strategy 1) to $E_{NS,SM,ADCP}$ = 0.79 ($E_{NS,SM,ADCP,5/95}$ = 0.6 – 0.74) using river geometry information obtained from a detailed field survey (Water level Strategy 2). The model performance also improved when increasing the number of virtual stations used for parameter selection. Therefore, in the absence of reliable discharge data as commonly the case in poorly or ungauged basins, altimetry data from multiple virtual stations combined with GRACE observations have the potential to fill this gap if combined with river geometry estimates.

### Acknowledgement

This research is supported by the TU Delft | Global Initiative, a program of the Delft University of Technology to boost Science and Technology for Global Development. This study would not have been possible without the help of those who provided us with the data. Local hydro-meteorological data was provided by WARMA (Water Resources Management Authority in Zambia), ZMD (Zambia Meteorological Department), GRDC (Global Runoff Data Centre) and NOAA (National Oceanic and Atmospheric Administration). Remotely sensed river water levels were obtained from DAHITI, HydroSat, EARPS and LEGOS.

### Literature

Abas, I.: Remote river rating in Zambia: A case study in the Luangwa river basin, Master of Science, Civil Engineering and Geosciences, Delft University of Technology, 2018.

https://doi.org/10.5194/hess-2019-346
Preprint. Discussion started: 10 September 2019


Hydrology and Earth System Sciences
Discussions

Ajami, N. K., Gupta, H., Wagener, T., and Sorooshian, S.: Calibration of a semi-distributed hydrologic model for streamflow estimation along a river system, Journal of Hydrology, 298, 112-135, 10.1016/j.jhydrol.2004.03.033, 2004.

Bauer-Gottwein, P., Jensen, I. H., Guzinski, R., Bredtoft, G. K. T., Hansen, S., and Michailovsky, C. I.: Operational river discharge forecasting in poorly gauged basins: The Kavango River basin case study, Hydrology and Earth System Sciences, 19, 1469-1485, 10.5194/hess-19-1469-2015, 2015.

Beilfuss, R., and dos Santos, D.: Patterns of Hydrological Change in the Zambezi Delta, Mozambique, in: Working Paper #2 Program for the Sustainable Management of Cahora Bassa Dam and the Lower Zambezi Valley, International Crane Foundation, Sofala, Mozambique, 2001.

Beven, K.: A manifesto for the equifinality thesis, Journal of Hydrology, 320, 18-36, https://doi.org/10.1016/j.jhydrol.2005.07.007, 2006.

Beven, K.: On doing better hydrological science, Hydrological Processes, 22, 3549-3553, 10.1002/hyp.7108, 2008.

Beven, K., and Westerberg, I.: On red herrings and real herrings: disinformation and information in hydrological inference, Hydrological Processes, 25, 1676-1680, 10.1002/hyp.7963, 2011.

Beven, K. J.: Preferential flows and travel time distributions: defining adequate hypothesis tests for hydrological process models, Hydrological Processes, 24, 1537-1547, 10.1002/hyp.7718, 2010.

Biancamaria, S., Frappart, F., Leleu, A. S., Marieu, V., Blumstein, D., Desjonquères, J.-D., Boy, F., Sottolichio, A., and Valle-Levinson, A.: Satellite radar altimetry water elevations performance over a 200m wide river: Evaluation over the Garonne River, Advances in Space Research, 59, 128-146, https://doi.org/10.1016/j.asr.2016.10.008, 2017.

Birkett, C. M.: Contribution of the TOPEX NASA Radar Altimeter to the global monitoring of large rivers and wetlands, Water Resources Research, 34, 1223-1239, 10.1029/98WR00124, 1998.

Birkinshaw, S. J., O'Donnell, G. M., Moore, P., Kilsby, C. G., Fowler, H. J., and Berry, P. A. M.: Using satellite altimetry data to augment flow estimation techniques on the Mekong River, Hydrological Processes, 24, 3811-3825, 10.1002/hyp.7811, 2010.

Bogning, S., Frappart, F., Blarel, F., Niño, F., Mahé, G., Bricquet, J. P., Seyler, F., Onguéné, R., Etamé, J., Paiz, M. C., and Braun, J. J.: Monitoring water levels and discharges using radar altimetry in an ungauged river basin: The case of the Ogooué, Remote Sensing, 10, 10.3390/rs10020350, 2018.

Calmant, S., Seyler, F., and Cretaux, J.: Monitoring Continental Surface Waters by Satellite Altimetry, 247-269 pp., 2009.

Clark, M. P., Nijssen, B., Lundquist, J. D., Kavetski, D., Rupp, D. E., Woods, R. A., Freer, J. E., Gutmann, E. D., Wood, A. W., Gochis, D. J., Rasmussen, R. M., Tarboton, D. G., Mahat, V., Flerchinger, G. N., and Marks, D. G.: A unified approach for process-based hydrologic modeling: 2. Model implementation and case studies, Water Resources Research, 51, 2515-2542, 10.1002/2015WR017200, 2015.

Clark, M. P., Schaefli, B., Schymanski, S. J., Samaniego, L., Luce, C. H., Jackson, B. M., Freer, J. E., Arnold, J. R., Moore, R. D., Istanbulluoglu, E., and Ceola, S.: Improving the theoretical underpinnings of process-based hydrologic models, Water Resources Research, 52, 2350-2365, 10.1002/2015WR017910, 2016.

AVISO+ Satellite Altimetry Data: www.aviso.altimetry.fr, last access: Jan 2018, Accessed 2018.

Danielson, J. J., and Gesch, D. B.: Global multi-resolution terrain elevation data 2010 (GMTED2010), Report 2011-1073, 2011.

de Oliveira Campos, I., Mercier, F., Maheu, C., Cochonneau, G., Kosuth, P., Blitzkow, D., and Cazenave, A.: Temporal variations of river basin waters from Topex/Poseidon satellite altimetry. Application to the Amazon



basin, Comptes Rendus de l'Académie des Sciences - Series IIA - Earth and Planetary Science, 333, 633-643, http://dx.doi.org/10.1016/S1251-8050(01)01688-3, 2001.

Demirel, M., Mai, J., Mendiguren González, G., Koch, J., Samaniego, L., and Stisen, S.: Combining satellite data and appropriate objective functions for improved spatial pattern performance of a distributed hydrologic model, 2018.

Drusch, M., Del Bello, U., Carlier, S., Colin, O., Fernandez, V., Gascon, F., Hoersch, B., Isola, C., Laberinti, P., Martimort, P., Meygret, A., Spoto, F., Sy, O., Marchese, F., and Bargellini, P.: Sentinel-2: ESA's Optical High-Resolution Mission for GMES Operational Services, Remote Sensing of Environment, 120, 25-36, https://doi.org/10.1016/j.rse.2011.11.026, 2012.

Satellite Missions Database: https://directory.eoportal.org/web/eoportal/satellite-missions, last access: Jan 2018, 2018.

Euser, T., Winsemius, H. C., Hrachowitz, M., Fenicia, F., Uhlenbrook, S., and Savenije, H. H. G.: A framework to assess the realism of model structures using hydrological signatures, Hydrology and Earth System Sciences, 17, 1893-1912, 10.5194/hess-17-1893-2013, 2013.

Euser, T., Hrachowitz, M., Winsemius, H. C., and Savenije, H. H. G.: The effect of forcing and landscape distribution on performance and consistency of model structures, Hydrological Processes, 29, 3727-3743, 10.1002/hyp.10445, 2015.

Fang, K., Shen, C., Fisher, J. B., and Niu, J.: Improving Budyko curve-based estimates of long-term water partitioning using hydrologic signatures from GRACE, Water Resources Research, 52, 5537-5554, 10.1002/2016WR018748, 2016.

Fleischmann, A., Siqueira, V., Paris, A., Collischonn, W., Paiva, R., Pontes, P., Crétaux, J. F., Bergé-Nguyen, M., Biancamaria, S., Gosset, M., Calmant, S., and Tanimoun, B.: Modelling hydrologic and hydrodynamic processes in basins with large semi-arid wetlands, Journal of Hydrology, 561, 943-959, 10.1016/j.jhydrol.2018.04.041, 2018.

Forootan, E., Khaki, M., Schumacher, M., Wulfmeyer, V., Mehrnegar, N., van Dijk, A. I. J. M., Brocca, L., Farzaneh, S., Akinluyi, F., Ramillien, G., Shum, C. K., Awange, J., and Mostafaie, A.: Understanding the global hydrological droughts of 2003–2016 and their relationships with teleconnections, Science of the Total Environment, 650, 2587-2604, 10.1016/j.scitotenv.2018.09.231, 2019.

Fovet, O., Ruiz, L., Hrachowitz, M., Faucheux, M., and Gascuel-Odoux, C.: Hydrological hysteresis and its value for assessing process consistency in catchment conceptual models, Hydrology and Earth System Sciences, 19, 105-123, 10.5194/hess-19-105-2015, 2015.

Frappart, F., Papa, F., Marieu, V., Malbeteau, Y., Jordy, F., Calmant, S., Durand, F., and Bala, S.: Preliminary Assessment of SARAL/AltiKa Observations over the Ganges-Brahmaputra and Irrawaddy Rivers, Marine Geodesy, 38, 568-580, 10.1080/01490419.2014.990591, 2015.

Freer, J., Beven, K., and Ambroise, B.: Bayesian Estimation of Uncertainty in Runoff Prediction and the Value of Data: An Application of the GLUE Approach, Water Resources Research, 32, 2161-2173, 10.1029/95WR03723, 1996.

Funk, C. C., Peterson, P. J., Landsfeld, M. F., Pedreros, D. H., Verdin, J. P., Rowland, J. D., Romero, B. E., Husak, G. J., Michaelsen, J. C., and Verdin, A. P.: A quasi-global precipitation time series for drought monitoring: U.S. Geological Survey, Data Series 832, 4, ftp://chg-ftpout.geog.ucsb.edu/pub/org/chg/products/CHIRPS-2.0/docs/USGS-DS832.CHIRPS.pdf, 2014.

Gao, H., Hrachowitz, M., Fenicia, F., Gharari, S., and Savenije, H. H. G.: Testing the realism of a topography-driven model (FLEX-Topo) in the nested catchments of the Upper Heihe, China, Hydrol. Earth Syst. Sci., 18, 1895-1915, 10.5194/hess-18-1895-2014, 2014.



Gao, H., Hrachowitz, M., Sriwongsitanon, N., Fenicia, F., Gharari, S., and Savenije, H. H. G.: Accounting for the influence of vegetation and landscape improves model transferability in a tropical savannah region, Water Resources Research, 52, 7999-8022, 10.1002/2016WR019574, 2016.

Garambois, P.-A., Calmant, S., Roux, H., Paris, A., Monnier, J., Finaud-Guyot, P., Samine Montazem, A., and Santos da Silva, J.: Hydraulic visibility: Using satellite altimetry to parameterize a hydraulic model of an ungauged reach of a braided river, Hydrological Processes, 31, 756-767, 10.1002/hyp.11033, 2017.

Garavaglia, F., Le Lay, M., Gottardi, F., Garçon, R., Gailhard, J., Paquet, E., and Mathevet, T.: Impact of model structure on flow simulation and hydrological realism: from a lumped to a semi-distributed approach, Hydrol. Earth Syst. Sci., 21, 3937-3952, 10.5194/hess-21-3937-2017, 2017.

Getirana, A. C. V., Bonnet, M.-P., Calmant, S., Roux, E., Rotunno Filho, O. C., and Mansur, W. J.: Hydrological monitoring of poorly gauged basins based on rainfall–runoff modeling and spatial altimetry, Journal of Hydrology, 379, 205-219, http://dx.doi.org/10.1016/j.jhydrol.2009.09.049, 2009.

Getirana, A. C. V.: Integrating spatial altimetry data into the automatic calibration of hydrological models, Journal of Hydrology, 387, 244-255, http://dx.doi.org/10.1016/j.jhydrol.2010.04.013, 2010.

Getirana, A. C. V., Bonnet, M. P., Rotunno Filho, O. C., Collischonn, W., Guyot, J. L., Seyler, F., and Mansur, W. J.: Hydrological modelling and water balance of the Negro River basin: evaluation based on in situ and spatial altimetry data, Hydrological Processes, 24, 3219-3236, 10.1002/hyp.7747, 2010.

Getirana, A. C. V., and Peters-Lidard, C.: Estimating water discharge from large radar altimetry datasets, Hydrol. Earth Syst. Sci., 17, 923-933, 10.5194/hess-17-923-2013, 2013.

Gharari, S., Hrachowitz, M., Fenicia, F., and Savenije, H. H. G.: Hydrological landscape classification: investigating the performance of HAND based landscape classifications ina central European meso-scale catchment, Hydrol. Earth Syst. Sci., 15, 3275-3291, 2011.

Gharari, S., Hrachowitz, M., Fenicia, F., and Savenije, H. H. G.: An approach to identify time consistent model parameters: sub-period calibration, Hydrol. Earth Syst. Sci., 17, 149-161, 10.5194/hess-17-149-2013, 2013.

Gharari, S., Hrachowitz, M., Fenicia, F., Gao, H., and Savenije, H. H. G.: Using expert knowledge to increase realism in environmental system models can dramatically reduce the need for calibration, Hydrol. Earth Syst. Sci., 18, 4839-4859, 10.5194/hess-18-4839-2014, 2014.

Gichamo, T. Z., Popescu, I., Jonoski, A., and Solomatine, D.: River cross-section extraction from the ASTER global DEM for flood modeling, Environmental Modelling & Software, 31, 37-46, https://doi.org/10.1016/j.envsoft.2011.12.003, 2012.

GlobCover, 2009.

Google Earth, 2018.

Gupta, H. V., Wagener, T., and Liu, Y.: Reconciling theory with observations: elements of a diagnostic approach to model evaluation, Hydrological Processes, 22, 3802-3813, 10.1002/hyp.6989, 2008.

Floods displace thousands in Mozambique: https://www.theguardian.com/world/2001/mar/28/mozambique.unitednations, last access: Jan 2017, 2001.

Hargreaves, G. H., and Samani, Z. A.: Reference Crop Evapotranspiration from Temperature, Applied Engineering in Agriculture, 1, 96-99, https://doi.org/10.13031/2013.26773, 1985.

Hargreaves, G. H., and Allen, R. G.: History and evaluation of hargreaves evapotranspiration equation, Journal of Irrigation and Drainage Engineering, 129, 53-63, 10.1061/(ASCE)0733-9437(2003)129:1(53), 2003.

Hasan, M. A., and Pradhanang, S. M.: Estimation of flow regime for a spatially varied Himalayan watershed using improved multi-site calibration of the Soil and Water Assessment Tool (SWAT) model, Environmental Earth Sciences, 76, 787, 10.1007/s12665-017-7134-3, 2017.

https://doi.org/10.5194/hess-2019-346
Preprint. Discussion started: 10 September 2019




Hrachowitz, M., Savenije, H. H. G., Blöschl, G., McDonnell, J. J., Sivapalan, M., Pomeroy, J. W., Arheimer, B., Blume, T., Clark, M. P., Ehret, U., Fenicia, F., Freer, J. E., Gelfan, A., Gupta, H. V., Hughes, D. A., Hut, R. W., Montanari, A., Pande, S., Tetzlaff, D., Troch, P. A., Uhlenbrook, S., Wagener, T., Winsemius, H. C., Woods, R. A., Zehe, E., and Cudennec, C.: A decade of Predictions in Ungauged Basins (PUB)—a review, Hydrological Sciences Journal, 58, 1198-1255, 10.1080/02626667.2013.803183, 2013.

Hrachowitz, M., Fovet, O., Ruiz, L., Euser, T., Gharari, S., Nijzink, R., Freer, J., Savenije, H. H. G., and Gascuel-Odoux, C.: Process consistency in models: The importance of system signatures, expert knowledge, and process complexity, Water Resources Research, 50, 7445-7469, 10.1002/2014WR015484, 2014.

Hrachowitz, M., and Clark, M. P.: HESS Opinions: The complementary merits of competing modelling philosophies in hydrology, Hydrol. Earth Syst. Sci., 21, 3953-3973, 10.5194/hess-21-3953-2017, 2017.

Hulsman, P., Bogaard, T. A., and Savenije, H. H. G.: Rainfall-runoff modelling using river-stage time series in the absence of reliable discharge information: a case study in the semi-arid Mara River basin, Hydrol. Earth Syst. Sci., 22, 5081-5095, 10.5194/hess-22-5081-2018, 2018.

Irons, J. R., Dwyer, J. L., and Barsi, J. A.: The next Landsat satellite: The Landsat Data Continuity Mission, Remote Sensing of Environment, 122, 11-21, https://doi.org/10.1016/j.rse.2011.08.026, 2012.

Jakeman, A. J., and Hornberger, G. M.: How much complexity is warranted in a rainfall-runoff model?, Water Resources Research, 29, 2637-2649, 10.1029/93WR00877, 1993.

Jian, J., Ryu, D., Costelloe, J. F., and Su, C.-H.: Towards hydrological model calibration using river level measurements, Journal of Hydrology: Regional Studies, 10, 95-109, https://doi.org/10.1016/j.ejrh.2016.12.085, 2017.

Jiang, L., Schneider, R., Andersen, O. B., and Bauer-Gottwein, P.: CryoSat-2 altimetry applications over rivers and lakes, Water (Switzerland), 9, 10.3390/w9030211, 2017.

Khaki, M., and Awange, J.: The application of multi-mission satellite data assimilation for studying water storage changes over South America, Science of the Total Environment, 647, 1557-1572, 10.1016/j.scitotenv.2018.08.079, 2019.

KlemeŠ, V.: Operational testing of hydrological simulation models, Hydrological Sciences Journal, 31, 13-24, 10.1080/02626668609491024, 1986.

Knutti, R.: Should we believe model predictions of future climate change?, Philosophical Transactions of the Royal Society A: Mathematical, Physical and Engineering Sciences, 366, 4647-4664, 10.1098/rsta.2008.0169, 2008.

Kouraev, A. V., Zakharova, E. A., Samain, O., Mognard, N. M., and Cazenave, A.: Ob' river discharge from TOPEX/Poseidon satellite altimetry (1992-2002), Remote Sensing of Environment, 93, 238-245, 10.1016/j.rse.2004.07.007, 2004.

Lakshmi, V.: The role of satellite remote sensing in the Prediction of Ungauged Basins, Hydrological Processes, 18, 1029-1034, 10.1002/hyp.5520, 2004.

Landerer, F. W., and Swenson, S. C.: Accuracy of scaled GRACE terrestrial water storage estimates, Water Resources Research, 48, 11, doi:10.1029/2011WR011453, 2012.

Leon, J. G., Calmant, S., Seyler, F., Bonnet, M. P., Cauhopé, M., Frappart, F., Filizola, N., and Fraizy, P.: Rating curves and estimation of average water depth at the upper Negro River based on satellite altimeter data and modeled discharges, Journal of Hydrology, 328, 481-496, 10.1016/j.jhydrol.2005.12.006, 2006.

Liu, G., Schwartz, F. W., Tseng, K. H., and Shum, C. K.: Discharge and water-depth estimates for ungauged rivers: Combining hydrologic, hydraulic, and inverse modeling with stage and water-area measurements from satellites, Water Resources Research, 51, 6017-6035, 10.1002/2015WR016971, 2015.

https://doi.org/10.5194/hess-2019-346
Preprint. Discussion started: 10 September 2019




Łyszkowicz, A. B., and Bernatowicz, A.: Current state of art of satellite altimetry, Geodesy and Cartography, 66, 259-270, https://doi.org/10.1515/geocart-2017-0016, 2017.

Manning, R.: On the flow of water in open channels and pipes, Transactions of the Institution of Civil Engineers of Ireland, 20, 161-207, 1891.

McMillan, H. K., and Westerberg, I. K.: Rating curve estimation under epistemic uncertainty, Hydrological Processes, 29, 1873-1882, 10.1002/hyp.10419, 2015.

Michailovsky, C. I., McEnnis, S., Berry, P. A. M., Smith, R., and Bauer-Gottwein, P.: River monitoring from satellite radar altimetry in the Zambezi River basin, Hydrol. Earth Syst. Sci., 16, 2181-2192, 10.5194/hess-16-2181-2012, 2012.

Michailovsky, C. I., Milzow, C., and Bauer-Gottwein, P.: Assimilation of radar altimetry to a routing model of the Brahmaputra River, Water Resources Research, 49, 4807-4816, 10.1002/wrcr.20345, 2013.

Michailovsky, C. I., and Bauer-Gottwein, P.: Operational reservoir inflow forecasting with radar altimetry: the Zambezi case study, Hydrol. Earth Syst. Sci., 18, 997-1007, 10.5194/hess-18-997-2014, 2014.

Montanari, M., Hostache, R., Matgen, P., Schumann, G., Pfister, L., and Hoffmann, L.: Calibration and sequential updating of a coupled hydrologic-hydraulic model using remote sensing-derived water stages, Hydrol. Earth Syst. Sci., 13, 367-380, 10.5194/hess-13-367-2009, 2009.

Nash, J. E., and Sutcliffe, J. V.: River flow forecasting through conceptual models part I — A discussion of principles, Journal of Hydrology, 10, 282-290, https://doi.org/10.1016/0022-1694(70)90255-6, 1970.

Nijzink, R. C., Samaniego, L., Mai, J., Kumar, R., Thober, S., Zink, M., Schäfer, D., Savenije, H. H. G., and Hrachowitz, M.: The importance of topography-controlled sub-grid process heterogeneity and semi-quantitative prior constraints in distributed hydrological models, Hydrol. Earth Syst. Sci., 20, 1151-1176, 10.5194/hess-20-1151-2016, 2016.

Nijzink, R. C., Almeida, S., Pechlivanidis, I. G., Capell, R., Gustafssons, D., Arheimer, B., Parajka, J., Freer, J., Han, D., Wagener, T., van Nooijen, R. R. P., Savenije, H. H. G., and Hrachowitz, M.: Constraining Conceptual Hydrological Models With Multiple Information Sources, Water Resources Research, 54, 8332-8362, 10.1029/2017WR021895, 2018.

Pandya, U., Patel, A., and Patel, D.: RIVER CROSS SECTION DELINEATION FROM THE GOOGLE EARTH FOR DEVELOPMENT OF 1D HEC-RAS MODEL-A CASE OF SABARMATI RIVER, GUJARAT, INDIA, International Conference on Hydraulics, Water Resources & Coastal Engineering, Ahmedabad, India, 2017.

Papa, F., Bala, S. K., Pandey, R. K., Durand, F., Gopalakrishna, V. V., Rahman, A., and Rossow, W. B.: Ganga-Brahmaputra river discharge from Jason-2 radar altimetry: An update to the long-term satellite-derived estimates of continental freshwater forcing flux into the Bay of Bengal, Journal of Geophysical Research: Oceans, 117, 10.1029/2012JC008158, 2012.

Paris, A., Dias de Paiva, R., Santos da Silva, J., Medeiros Moreira, D., Calmant, S., Garambois, P. A., Collischonn, W., Bonnet, M. P., and Seyler, F.: Stage-discharge rating curves based on satellite altimetry and modeled discharge in the Amazon basin, Water Resources Research, 52, 3787-3814, 10.1002/2014WR016618, 2016.

Pechlivanidis, I. G., and Arheimer, B.: Large-scale hydrological modelling by using modified PUB recommendations: The India-HYPE case, Hydrology and Earth System Sciences, 19, 4559-4579, 10.5194/hess-19-4559-2015, 2015.

Pedinotti, V., Boone, A., Decharme, B., Crétaux, J. F., Mognard, N., Panthou, G., Papa, F., and Tanimoun, B. A.: Evaluation of the ISBA-TRIP continental hydrologic system over the Niger basin using in situ and satellite derived datasets, Hydrology and Earth System Sciences, 16, 1745-1773, 10.5194/hess-16-1745-2012, 2012.



Pereira-Cardenal, S. J., Riegels, N. D., Berry, P. A. M., Smith, R. G., Yakovlev, A., Siegfried, T. U., and Bauer-Gottwein, P.: Real-time remote sensing driven river basin modeling using radar altimetry, Hydrol. Earth Syst. Sci., 15, 241-254, 10.5194/hess-15-241-2011, 2011.

Pramanik, N., Panda, R. K., and Sen, D.: One Dimensional Hydrodynamic Modeling of River Flow Using DEM Extracted River Cross-sections, Water Resour Manage, 24, 835-852, 10.1007/s11269-009-9474-6, 2010.

Prenner, D., Kaitna, R., Mostbauer, K., and Hrachowitz, M.: The Value of Using Multiple Hydrometeorological Variables to Predict Temporal Debris Flow Susceptibility in an Alpine Environment, Water Resources Research, 54, 6822-6843, 10.1029/2018WR022985, 2018.

Rakovec, O., Kumar, R., Attinger, S., and Samaniego, L.: Improving the realism of hydrologic model functioning through multivariate parameter estimation, Water Resources Research, 52, 7779-7792, 10.1002/2016WR019430, 2016.

Rantz, S. E.: Measurement and computation of streamflow: Volume 2, Computation of Discharge, Report 2175, 1982.

Rennó, C. D., Nobre, A. D., Cuartas, L. A., Soares, J. V., Hodnett, M. G., Tomasella, J., and Waterloo, M. J.: HAND, a new terrain descriptor using SRTM-DEM: Mapping terra-firme rainforest environments in Amazonia, Remote Sensing of Environment, 112, 3469-3481, https://doi.org/10.1016/j.rse.2008.03.018, 2008.

Revilla-Romero, B., Beck, H. E., Burek, P., Salamon, P., de Roo, A., and Thielen, J.: Filling the gaps: Calibrating a rainfall-runoff model using satellite-derived surface water extent, Remote Sensing of Environment, 171, 118-131, http://dx.doi.org/10.1016/j.rse.2015.10.022, 2015.

SADC: Integrated Water Resources Management Strategy and Implementation Plan for the Zambezi River Basin, Euroconsult Mott MacDonald, 2008.

Santhi, C., Kannan, N., Arnold, J. G., and Di Luzio, M.: Spatial Calibration and Temporal Validation of Flow for Regional Scale Hydrologic Modeling, JAWRA Journal of the American Water Resources Association, 44, 829-846, 10.1111/j.1752-1688.2008.00207.x, 2008.

Savenije, H. H. G.: Equifinality, a blessing in disguise?, Hydrological Processes, 15, 2835-2838, 10.1002/hyp.494, 2001.

Savenije, H. H. G.: Topography driven conceptual modelling (FLEX-Topo), Hydrol. Earth Syst. Sci., 14, 2681-2692, 2010.

Sawicz, K., Wagener, T., Sivapalan, M., Troch, P. A., and Carrillo, G.: Catchment classification: Empirical analysis of hydrologic similarity based on catchment function in the eastern USA, Hydrology and Earth System Sciences, 15, 2895-2911, 10.5194/hess-15-2895-2011, 2011.

Schleiss, A. J., and Matos, J. P.: Chapter 98: Zambezi River Basin, in: Chow's Handbook of Applied Hydrology, edited by: Singh, V. P., McGraw-Hill Education - Europe, United States, 2016.

Schneider, R., Godiksen, P. N., Villadsen, H., Madsen, H., and Bauer-Gottwein, P.: Application of CryoSat-2 altimetry data for river analysis and modelling, Hydrol. Earth Syst. Sci., 21, 751-764, 10.5194/hess-21-751-2017, 2017.

Schoups, G., Lee Addams, C., and Gorelick, S. M.: Multi-objective calibration of a surface water-groundwater flow model in an irrigated agricultural region: Yaqui Valley, Sonora, Mexico, Hydrol. Earth Syst. Sci., 9, 549-568, 10.5194/hess-9-549-2005, 2005.

Schumann, G., Kirschbaum, D., Anderson, E., and Rashid, K.: Role of Earth Observation Data in Disaster Response and Recovery: From Science to Capacity Building, in: Earth Science Satellite Applications edited by: Hossain, F., Springer International Publishing, Seattle, USA, 2016.



965 Schwatke, C., Dettmering, D., Bosch, W., and Seitz, F.: DAHITI – an innovative approach for estimating water level time series over inland waters using multi-mission satellite altimetry, Hydrol. Earth Syst. Sci., 19, 4345-4364, 10.5194/hess-19-4345-2015, 2015.

Seibert, J., and Beven, K. J.: Gauging the ungauged basin: how many discharge measurements are needed?, Hydrol. Earth Syst. Sci., 13, 883-892, 10.5194/hess-13-883-2009, 2009.

970 Seibert, J., and Vis, M. J. P.: How informative are stream level observations in different geographic regions?, Hydrological Processes, 30, 2498-2508, 10.1002/hyp.10887, 2016.

Seyler, F., Calmant, S., Silva, J. S. d., Moreira, D. M., Mercier, F., and Shum, C. K.: From TOPEX/Poseidon to Jason-2/OSTM in the Amazon basin, Advances in Space Research, 51, 1542-1550, https://doi.org/10.1016/j.asr.2012.11.002, 2013.

975 Sikorska, A. E., and Renard, B.: Calibrating a hydrological model in stage space to account for rating curve uncertainties: general framework and key challenges, Advances in Water Resources, 105, 51-66, https://doi.org/10.1016/j.advwatres.2017.04.011, 2017.

Smith, B., and Sandwell, D.: Accuracy and resolution of shuttle radar topography mission data, Geophysical Research Letters, 30, 10.1029/2002GL016643, 2003.

980 Spearman, C.: The proof and measurement of association between two things, The American Journal of Psychology, 15, 72-101, 1904.

Sulistioadi, Y. B., Tseng, K. H., Shum, C. K., Hidayat, H., Sumaryono, M., Suhardiman, A., Setiawan, F., and Sunarso, S.: Satellite radar altimetry for monitoring small rivers and lakes in Indonesia, Hydrol. Earth Syst. Sci., 19, 341-359, 10.5194/hess-19-341-2015, 2015.

985 Sun, W., Ishidaira, H., and Bastola, S.: Calibration of hydrological models in ungauged basins based on satellite radar altimetry observations of river water level, Hydrological Processes, 26, 3524-3537, 10.1002/hyp.8429, 2012.

Sun, W., Ishidaira, H., Bastola, S., and Yu, J.: Estimating daily time series of streamflow using hydrological model calibrated based on satellite observations of river water surface width: Toward real world applications, 990 Environmental Research, 139, 36-45, http://dx.doi.org/10.1016/j.envres.2015.01.002, 2015.

Sun, W., Fan, J., Wang, G., Ishidaira, H., Bastola, S., Yu, J., Fu, Y. H., Kiem, A. S., Zuo, D., and Xu, Z.: Calibrating a hydrological model in a regional river of the Qinghai–Tibet plateau using river water width determined from high spatial resolution satellite images, Remote Sensing of Environment, 214, 100-114, https://doi.org/10.1016/j.rse.2018.05.020, 2018.

995 Swenson, S. C., and Wahr, J.: Post-processing removal of correlated errors in GRACE data, Geophys. Res. Lett., 33, doi:10.1029/2005GL025285, 2006.

Swenson, S. C.: GRACE monthly land water mass grids NETCDF RELEASE 5.0, in, PO.DAAC, CA, USA, 2012.

Tang, Y., Hooshyar, M., Zhu, T., Ringler, C., Sun, A. Y., Long, D., and Wang, D.: Reconstructing annual 1000 groundwater storage changes in a large-scale irrigation region using GRACE data and Budyko model, Journal of Hydrology, 551, 397-406, https://doi.org/10.1016/j.jhydrol.2017.06.021, 2017.

Tarpanelli, A., Barbetta, S., Brocca, L., and Moramarco, T.: River discharge estimation by using altimetry data and simplified flood routing modeling, Remote Sensing, 5, 4145-4162, 10.3390/rs5094145, 2013.

Tarpanelli, A., Amarnath, G., Brocca, L., Massari, C., and Moramarco, T.: Discharge estimation and forecasting 1005 by MODIS and altimetry data in Niger-Benue River, Remote Sensing of Environment, 195, 96-106, 10.1016/j.rse.2017.04.015, 2017.

The World Bank: The Zambezi River Basin: A Multi-Sector Investment Opportunities Analysis, in, 2010.

https://doi.org/10.5194/hess-2019-346
Preprint. Discussion started: 10 September 2019


Hydrology and Earth System Sciences
Discussions

Tourian, M. J., Sneeuw, N., and Bárdossy, A.: A quantile function approach to discharge estimation from satellite altimetry (ENVISAT), Water Resources Research, 49, 2013.

Tourian, M. J., Tarpanelli, A., Elmi, O., Qin, T., Brocca, L., Moramarco, T., and Sneeuw, N.: Spatiotemporal densification of river water level time series by multimission satellite altimetry, Water Resources Research, 52, 1140-1159, 10.1002/2015WR017654, 2016.

Tourian, M. J., Schwatke, C., and Sneeuw, N.: River discharge estimation at daily resolution from satellite altimetry over an entire river basin, Journal of Hydrology, 546, 230-247, https://doi.org/10.1016/j.jhydrol.2017.01.009, 2017.

University of East Anglia Climatic Research Unit, Harris, I. C., and Jones, P. D.: CRU TS4.01: Climatic Research Unit (CRU) Time-Series (TS) version 4.01 of high-resolution gridded data of month-by-month variation in climate (Jan. 1901- Dec. 2016), Centre for Environmental Data Analysis,, doi:10.5285/58a8802721c94c66ae45c3baa4d814d0, 2017.

Velpuri, N. M., Senay, G. B., and Asante, K. O.: A multi-source satellite data approach for modelling Lake Turkana water level: calibration and validation using satellite altimetry data, Hydrol. Earth Syst. Sci., 16, 1-18, 10.5194/hess-16-1-2012, 2012.

Winsemius, H. C., Savenije, H. H. G., and Bastiaanssen, W. G. M.: Constraining model parameters on remotely sensed evaporation: justification for distribution in ungauged basins?, Hydrol. Earth Syst. Sci., 12, 1403-1413, 10.5194/hess-12-1403-2008, 2008.

ZAMCOM, SADC, and SARDC: Zambezi Environment Outlook 2015, Harare, Gaborone, 2015.

Zhou, X., and Wang, H.: Application of Google Earth in Modern River Sedimentology Research, 1-8 pp., 2015.

Zink, M., Mai, J., Cuntz, M., and Samaniego, L.: Conditioning a Hydrologic Model Using Patterns of Remotely Sensed Land Surface Temperature, Water Resources Research, 54, 2976-2998, 10.1002/2017WR021346, 2018.